Department of Precision and Microsystems Engineering

Manufacturing of the fully Inkjet-printed Dielectric Elastomer Actuators

Yantong Wu

Report no : 2022.040
Coach : Dr. Ir. M. Tichem; Dr. A. Hunt
Specialisation : MNE
Type of report : Master Thesis
Date : 18 July 2022

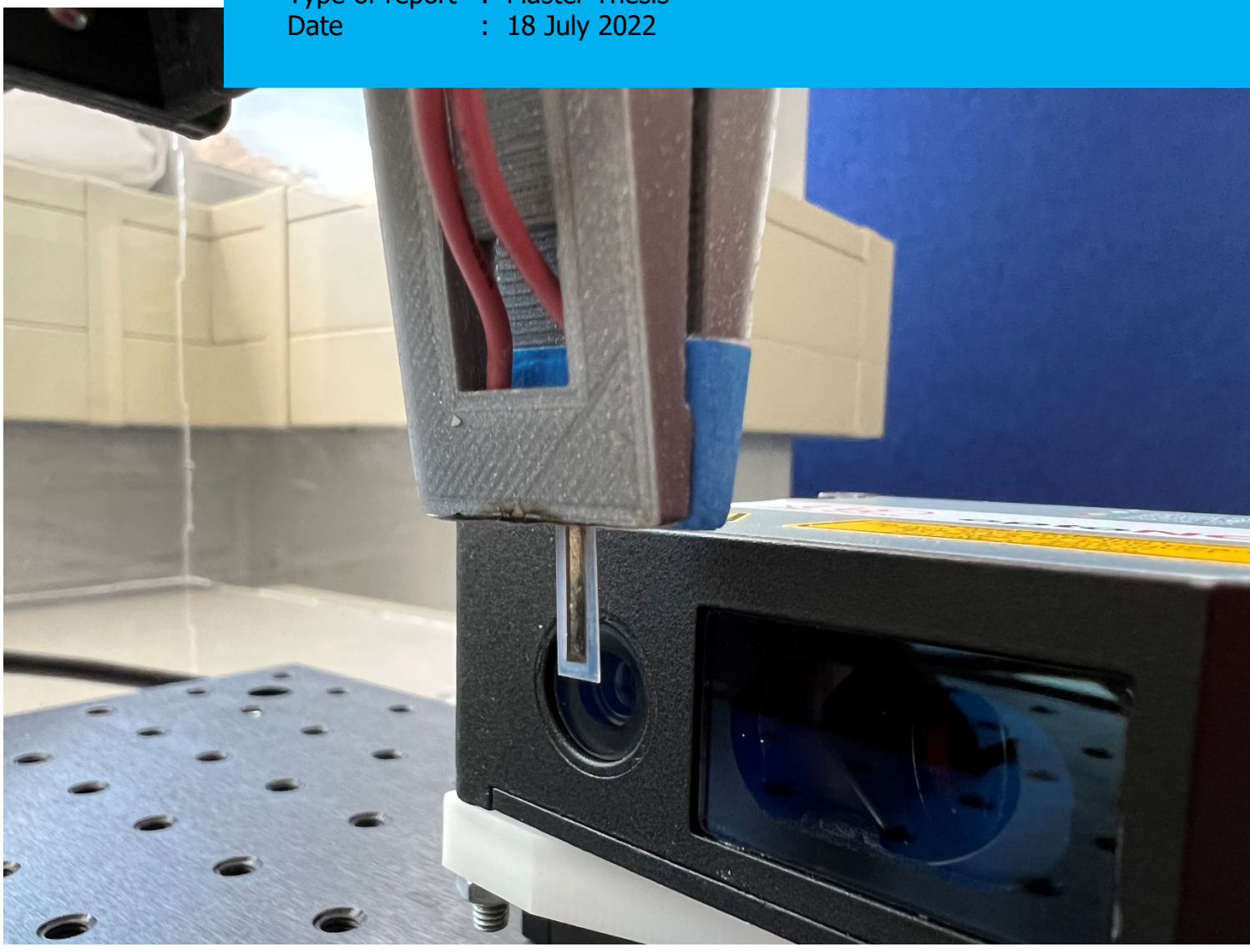

TU Delft Delft University of Technology

Challenge the future

Manufacturing of the fully Inkjet-printed Dielectric Elastomer Actuators

by

Yantong Wu

to obtain the degree of
Master of Science
in Mechanical Engineering
Delft University of Technology
July 18, 2022.

Student number:	5238803	
Project duration:	September, 2021 – July, 2022	
Thesis committee:	Dr. Ir. M. Tichem,	TU Delft, Seniorsupervisor, Chair
	Dr. A. Hunt,	TU Delft, Supervisor
	Dr. M. Mastrangeli,	TU Delft
	Dr. D. Farhadi Machekposhti,	TU Delft

This thesis is confidential and cannot be made public until July 2024.

TU Delft

Acknowledgements

For the last 11 months I took a lot of dedication, and patience, I'm glad finally everything goes as expected. Now I'm writing this one final page of the contribution, my master thesis, and I'd like to thank several people who have been there with me along the way.
First I'd like to thank Andres Hunt, my supervisor, for the guidance and support in every single aspect of the project process, from printer to measurement setup; the 3mE lab technicians for their support during the experiments; Marcel Tichem for the treasure advice and brainstorming during every meeting we had; and every staff in the lab that gave device training to me.
Besides the staff supporting this research, I've also been lucky enough to have friends and family supporting me and listening to my frustrating thoughts whenever it was necessary. I'd like to thank my mommy and daddy, they support me without any conditions at every point in life. I'd like to also thank my friends met in the Netherlands, Shawn, Zhou, Dorothea, Thorkell, Victor, Zhichao, Houman, Jeoren... They lift me up during my time studying and living in Delft. And last but not least, thank you to my closest friends across the world for supporting me without time limit, Taotao, Zou, Bing, Shuxin, and J.L.

Yantong Wu
Delft, July 18, 2022

Abstract

This thesis aims to solve the problems and fabricate fully inkjet-printed dielectric elastomer actuators with silver electrodes and a PDMS middle layer. First, a conductive silver electrode is printed on a coated PET substrate, followed by a printing of the dielectric elastomer middle layer to cover the bottom electrode. Then, the top silver layer is printed on the PDMS to achieve the top electrode. The problems intended to be solved in this work include printing the dielectric elastomer middle layer, treating the PDMS layer, the significant surface cracking, and the non-conductivity of the top electrode. During the fabrication process, different concentrations of PDMS solution are tested printing. Observations on these printed samples are made to validate the most suitable printing solution and printing process/settings. Different surface treatment cycles for the PDMS layer are also adopted to determine the most suitable one, what effect is brought to the PDMS layer surface, and how they influence the top electrode. For the fabrication of the top electrodes, experiments are accomplished and repeated, coming with failures, which will be presented and discussed later. Lastly, displacement and frequency response measurements are essential to check the performance of the DEAs, being critical sections of the thesis.

Contents

1 Introduction

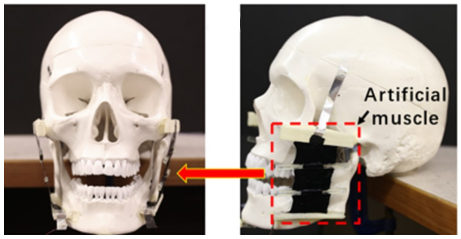

Figure 1.1. Robot driven by artificial muscles to mimic human jaw motion [1].

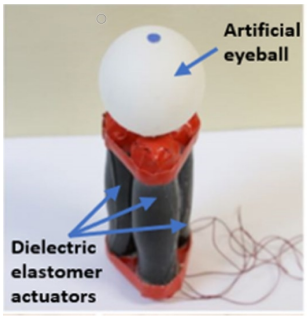

Figure 1.2. Artificial eyeball driven by three spring roll soft actuators [2].

An actuator is a mechanical device for moving or controlling a mechanism or system, including pneumatic actuators, electronic actuators, motors, and hydraulic cylinders [3]. However, the weight, limited size, complex transmission, and shape of such actuators restrict their application in some cases. These have indead led to investigation of alternative technologies for various applications. Smart materials are developed with one or more properties that can be significantly changed in a controlled manner by an externally applied field. Their characteristics are reversible and consequently guarantee actuation and sensing functions. Compared to conventional actuators, such actuators are relatively high integrated. They can be applied not just to be a discrete part of the system; they serve as the system itself, combining sensing, actuation, and mechanical functions [4]. Electroactive polymers are robust materials for implementing a flexible actuation mechanism in soft actuators. As a type of EAP, the dielectric elastomer can work as a soft actuator driven by the effective electrostriction between compliant electrodes. They are capable of large strains and response times below 1ms, but they require driving voltage in the kV range, limiting the possible applications. Luckily, low actuation voltage DEAs require low stiffness and thin elastomer layers and are easier and cheaper to implement due to the lower voltage requirements. It is suitable to drive compliant devices on micro and nano scales as an actuation mechanism. The lightweight, flexibility with non-geometric constraints, cost-effectiveness, and fast response provide chances for dielectric elastomer actuators configured in various shapes to enlarge their potential as artificial muscle [5], such as human jaw motion [1], eyeball movement [2], as well as soft robots [6]. One way to obtain low voltage driven DEAs is to decrease the dielectric layer thickness, typically in the 20–100μm range; the other way is to have optimized material properties [7]. Therefore, fabrication for low actuation voltage DEAs is feasible, especially applying the inkjet printing method, a fabrication technique with less complexity and no need for a mask.

Among various fabrication methods such as chemical vapor deposition, etching, and UV-lithography, inkjet printing stands out for relatively fast printing speed, less complexity, different layers with desirable configurations, and mask-free material deposition. Although inkjet printing only allows a small amount of material to pass through the nozzle, and the print head is less durable, prone to clogging and damage, the advantages are still attractive and lead to the flourishing development of inkjet printing DEAs. The application of inkjet printing include producing circuits [8], microfluidic devices [9], biochemical applications [10] and lab-on-a-chip community [11].
When talking about the existing DEAs, some stacked DEAs were successfully fabricated, applying methods such as spin-coating [12], cutting and piling up [13], spray deposition [14], and folding [15]. However, applying the inkjet printing method to fabricate the single layer DEAs was not ideally successful [16]. In addition, some defects, such as surface cracking, high resistance, and non-adhesion (top electrode to dielectric polymer) phenomena, happened in DEAs during and after the fabrication process. Therefore, the application of inkjet printing in manufacturing DEA remains to be explored, leading it to become the primary goal of this thesis project.

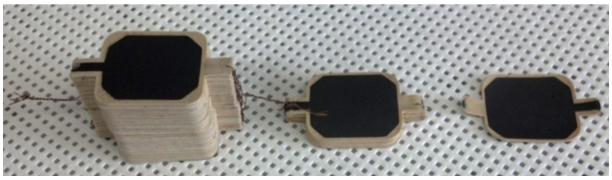

Figure 1.3. Stack unit DEAs form into a multistacked actuator [13].

This research aims to solve the problems in the fully inkjet-printed DEA fabrication process and print in different geometries while achieving insights into the requirements, limitations, and results of each fabrication step involved. In the end, a functional prototype of DEA is expected. The challenges include inkjet printing smooth PDMS layers with self-prepared PDMS solution, solving the non-adhesion problem of the top silver electrode to the PDMS layer, the surface morphology/quality of the top silver electrode, and the conductivity issue for it. The interactions between the different components that build the actuators were not examined. These involved using different silver nanoparticle inks to fabricate electrodes, examining the surface treatment methods, observing the appearance/surface of different layers after each manufacturing step, and testing conductivity and displacement performance of actuators.
Several (fabrication) **challenges** that are intended to be solved in this thesis project include:

1. Inkjet printing the PDMS dielectric layer.
2. Solving the problems in surface treatment of getting the smooth and hydrophilic PDMS surface that allows silver ink adhesion.
3. Solving the problem in obtaining the low-resistance silver electrodes.
4. Solving the problem in the top electrode that has huge cracks affecting conductivity.
5. Fabricating functional single-layer DEAs.

The results of the conducted research are detailed in this report, and this thesis is organized into four parts. The following chapters concern the individual components of the single-layer and multi-layer DEAs, materials and methods, results, and the observations of each layer during the experimental processes involved in creating the component. First, the working principles and structures of DEAs will be presented in section 2.1 of chapter 2. The manufacturing process and characterization of measurement setup will be introduced in the following section 2.2 and section 2.3, demonstrating the possibility of producing the inkjet-printed electrodes and dielectric films, as well as the suitability of inkjet-printed DE films for use with dielectric elastomer actuators. (External) Factors that influence the experiment

process and results will be described. The chapter 3 will present the manufacturing results of each layer and show the success and the attempts to gain ”perfect” layers. In the section 3.1 in this chapter, the surface morphology and printing results of different samples will be compared to check the feasibility of each manufacturing step. Critical testing results of prototype DEAs will be presented in the following section 3.2. The measurement test for the displacement of actuators was done with sinusoidal waves in different frequencies and amplitudes. Finally, the report is concluded with an overview of the obtained results and their discussion chapter 4, ending with conclusions for the project and recommendations for future research and directions in improving the printing process and performance of DEAs in chapter 5 and chapter 6.

2

Materials and Methods

2.1. Structure, working principle, and design of DEAs

In this section, structures, working principles, and the single-layer design of DEAs will be introduced sequentially. DEAs are soft actuators that can show displacement when an electric field is applied. Due to the electrostatic force induced by opposite charges, the electrodes will compress the elastomer membrane lying in between. Therefore, the elastomer in the single-layer DEA is vertically compressed and laterally expanded, as shown in Figure 2.1. The working principle in the multi-layer DEA is the same, and the structure of a typical multi-layer DEA is shown in Figure 2.2.

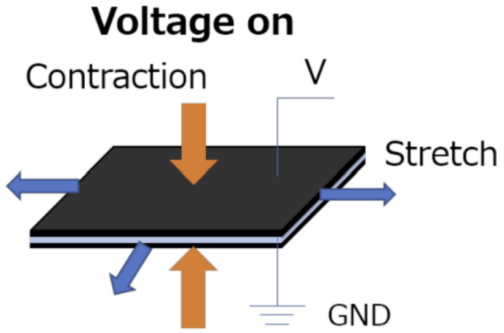

Figure 2.1. Driving principle of the single-layer dielectric elastomer actuator [17].

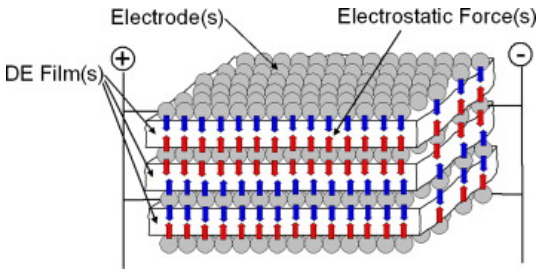

Figure 2.2. A layered composite structure of a stacked DEA composed of electrodes and DE film layers [18].

The compressive stress of a single set of DEA can be related to the elastic compressive strain s_z of a DEA as follows:

$$s_z = -\frac{p}{Y} = -\frac{\epsilon_0 \epsilon_r}{Y}\left(\frac{V}{z}\right)^2 \tag{2.1}$$

Then for the elastic compressive strain s_{sz} of a stacked DEA, the expression is [12]:

$$s_{sz} = n s_z \tag{2.2}$$

where the absolute deformation is n times higher than the deformation of a single film.
For small deformations and ignoring the stiffening impact of the electrodes, the lateral strains $s_x = s_y$ can be approximated by [7]

$$s_x = -\frac{s_z}{2} \tag{2.3}$$

This study aims to produce a unimorph design to obtain the induced strain (bending motion) of DEAs. A unimorph is a cantilever that consists of one active layer and one passive layer. The application of an electric field induces deformation in the active layer. This deformation induces a bending displacement in the cantilever. In this case, the unimorph design consists of dielectric elastomer layers and compliant electrodes. As a result, the unimorph can remain in an almost straight neutral position when it is not electrically activated. However, the active layers elongate upon electrical activation. Consequently, the unimorph will bend towards the side of the passive layer (in this case, the substrate), as shown in Figure 2.3.

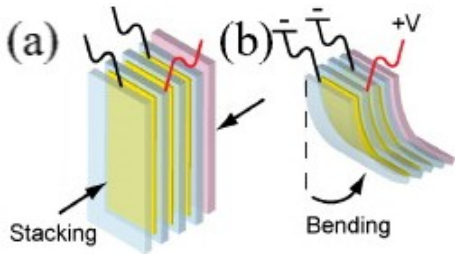

Figure 2.3. Multi-layered dielectric elastomer unimorph : (a) stack of component layers; (b) activation of multi-layered elastomeric unimorph [19].

The unimorph design of each layer is shown in Figure 2.4, divided into four layers, the substrate (passive layer), the bottom electrode, the middle dielectric polymer layer, and the top electrode. The active layer is the metalized dielectric elastomer layer. The unimorph design is simple, easy to be drawn in Inkscape, and no dimensions are shown since the sizes can be adjusted in the printer software, which will be introduced later. One vital aspect is that the middle polymer layer should be larger than the bottom and top layers. This action can guarantee the electrical and mechanical isolation between the bottom and the top electrodes.

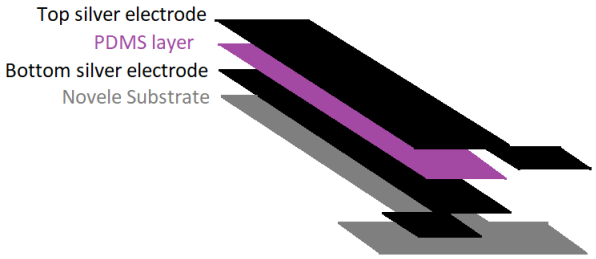

Figure 2.4. Structure of different layers in the single layer DEA.

2.2. Actuator Materials and methods

This section will introduce details by several subsections; the chemicals for PDMS solution and the used silver inks will be included in subsection 2.2.1; details of the equipment that will be used for fabrication and observation will be introduced in subsection 2.2.2; and printing settings and steps will be detailed in subsection 2.2.3 and Appendix A.

2.2.1. Reagents and Materials

SYLGARD^{TM}184 Silicone Elastomer Base, Dow Corning [20] is prepared in a 10:1 base-catalyst (curing agent) ratio based on the instructions of Dow Inc. Base and catalyst is stirred in a glass beaker for approximately 5 minutes. For inkjet printing PDMS solution, desiring is not required. Therefore, in this case, the octyl acetate CH3CO2(CH2)7CH3, Sigma Aldric [21], Mexico, is directly added to the mixture

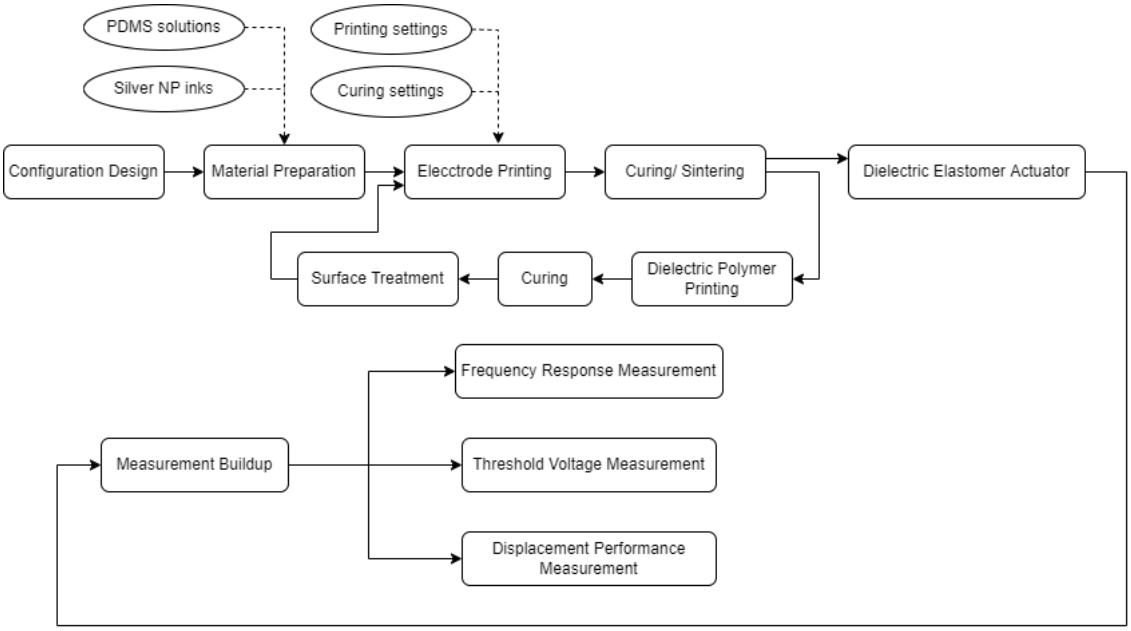

Figure 2.5. Manufacturing loop and measurement process for the fully inkjet-printed dielectric elastomer actuator.

at weight ratios of 1:4, 1:2, and 1:1 in glass beakers. The final mixtures are stirred for approximately 3 minutes. Then the solutions were filled in the DMC-11610 cartridges. The glass beakers should be cleaned with IPA and dried with the air gun afterward.
Two types of silver inks were applied to fabricate different silver layers (Mitsubishi NBSIJ-MU01, NovaCentrix JS-A211), depending on laying on porous (Novele PET) or non-porous (polymer layer) substrates. Silver nanoparticle (Ag NP) inks (NBSIJ-MU01, Mitsubishi [22] and JS-A211 (40% Ag), Novacentrix [23]) purchased from commercial market for printing were filled in the DMC-11610 cartridges.
The substrate used for printing is a coated PET sheet Novele IJ-220, NovaCentrix.

2.2.2. Apparatus

A Pixdro Printer LP50 inkjet printer, Suss-MicroTec [24], is used; the PIXDRO HMI Software is used to input the control settings and figures to print; a print head set up KONICA MINOLTA 512 is used to test and get familiar with droplet control; the DMC print head (Meyer Burger) and the 10pL cartridge DMC-11610, FUJIFILM $\mathrm{Dimatix}^{\mathrm{TM}}$, Inc., are assembled to print Ag NP inks and the PDMS layers.
An optical microscope (KEYENCE), a white light interference microscope (Bruker), and a scanning electron microscope were used to obtain images and determine the geometrical area of the printed electrode and the polymer layer. KEYENCE was used to check the morphology of silver tracks, which can give clear, labeled pictures with models of lenses and a scale bar. The white light interference microscope Bruker was used to check the morphological details and the height of conductive layers, which can provide data set and 3d profiles. With a scanning electron microscope, the cross-section of the samples can be observed, therefore, measuring the thickness of transparent polymer layers.

2.2.3. Printer settings and steps

The PiXDRO LP50 is used for practical applications in this project. The parameters such as printing speed and direction should be adjusted to control the printing. The general printing steps of each layer in DEAs consist:

- Preparing and placing the print head in the correct position on the printer.
- Filling the cartridges that fit the specific print head.

- Having substrates prepared.
- Adjusting the printing settings, including waveform for different inks/materials.
- Cleaning up the substrate table and storing the print head.

Basic settings and step details in printing are expanded in Appendix A.

2.2.4. Actuator fabrication

The fabrication of dielectric elastomer actuators can be divided into mainly three layers: bottom electrodes, dielectric elastomer layers, and top electrodes.

bottom electrode fabrication: After the AgNP ink had been injected into a 10 pL DMC-11610 cartridge, the printing process was carried out at room temperature, and cleaning cycles (purging) were used before printing. Only one nozzle was activated to print, and two layers of ink were necessary to obtain a conductive silver film on substrates. The silver ink for the bottom electrode is self-sintered during the printing process, but the substrate table can be heated up at 35°C to ensure speeding up the solvent evaporation. The printing settings and waveform of these two types of silver ink were shown in Table A.1, and Figure A.2(b).

Dielectric elastomer layer fabrication: Once the PDMS solution was prepared well, it was jetted into the cartridge reservoir using a filter and needle. The solution should be used up or cleaned after 4 days maximum of preparation; otherwise, it can cure and block the cartridge. The PDMS solution should be printed at a relatively high voltage due to its high viscosity compared to silver inks. The printhead of the PDMS solution should also avoid being heated up for a long time, preventing unexpected polymer curing. The printing process was carried out at room temperature, and cleaning cycles were applied before printing. Only one nozzle was activated, and 2 layers of polymer were printed. Multiple polymer layers are added to ensure full insulation between the top and bottom electrodes. The first layer of PDMS should have been immediately (semi-)cured during printing with a heated substrate table at 80°C. Before the second layer is printed, the first layer of PDMS should rest on the substrate for at least 5 min to ensure the (semi-)cured state, allowing better coverage for the second layer of polymer; this is also required for not over-heating the print head. When the second layer printing finishes, the sample should be held in an oven at about 80°C for at least 2h to cure the PDMS layers and solvent evaporation fully. The curing temperature must not exceed the glass transition point of the PDMS (T_g<150°C). All post-processing steps for silver inks consisting of purely thermal treatments should be below this point.

Top electrode fabrication: The printing process for the top electrodes was carried out at room temperature, and cleaning cycles (purging) were used before printing. Only one nozzle was activated to print, and 2 layers were necessary to obtain a well-adhesive conductive layer on polymer. The silver ink for the top electrode was cured at 40°C during printing plus 30min after the printing process; the top electrodes were sintered under UV light; UV light can be the UV module integrated into the printer or an extra UV light setup. In this case, an extra UV light setup is more powerful to sinter the top electrode, with 1min exposure time. The printing settings and waveform for the top electrode were shown in A.2(c). Essential settings are listed in Table 2.1.

2.3. Characterization of Manufactured Sample and Measurement

In this work, the single-layer dielectric elastomer actuators were manufactured based on a 4-layer structure set in which all layers are applied sequentially as shown in Figure 2.4. The layers from bottom to top are the PET substrate, the printed bottom electrode, the inkjet-printed PDMS, and the printed top electrode. For the characterization of the measurement setup, details will be included in subsection 2.3.1

Table 2.1: Essential settings in fabricating layers in DEAs.

Functional Layer	Bottom electrode	Dielectric elastomer layer	Top electrode
Number of nozzle	1	1	1
Driven voltage / V	60	80	60
Substrate temperature / °C	35	80	40
Cartridge temperature / °C	28	35-50	28
Number of layer	2	2	2
Curing time	Immediately	Printing time + 2h	Printing time + 30min
Sintering	Selft-sinter	N/A	1min UV sintering

2.3.1. Measurement setup

In order to characterize the performance of actuators, it is necessary to measure the steady-state deflection with an excitation and measurement setup. Therefore, a laser sensor module (OptoNCDT 1750, Micro-epsilon [25]), a data acquisition device (USB-6211, National Instruments [26]), a voltage amplifier (HVA1500/50, Smart Material [27]), a safety acrylic cover, and hardware for setup skeleton was used to build up the measurement setup.

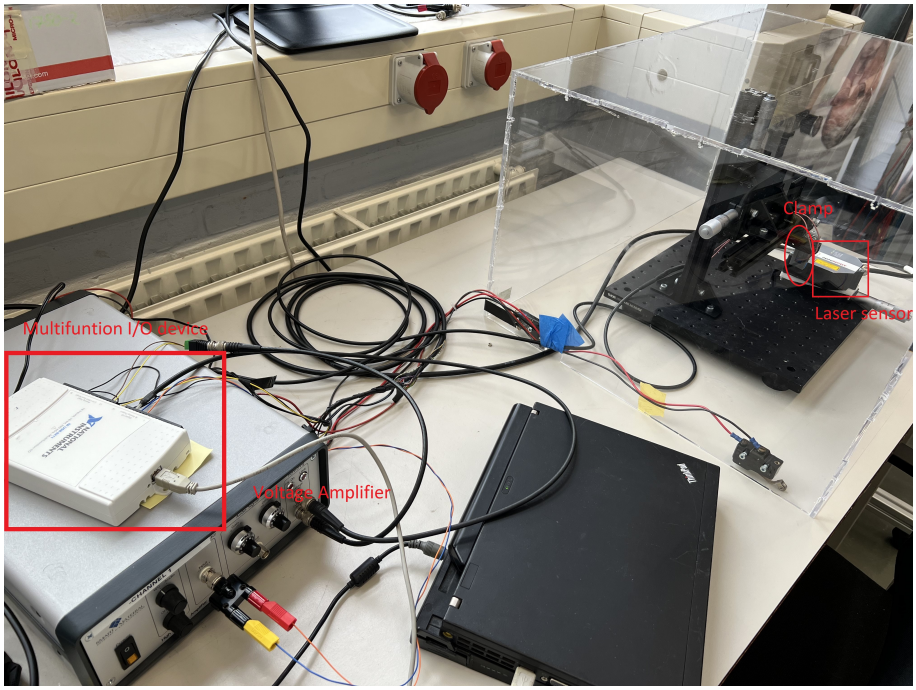

Figure 2.6. Measurement setup structure for actuator characterization.

The connection diagram and the picture of the measurement setup are shown in Figure 2.7 and Figure 2.6. Measurements for deflection with voltage sources are taken with a setup consisting of a Multifunction I/O device fed into a high voltage amplifier. The amplifier amplifies the input voltage signal and is connected directly to the contact pads of the actuators via a clamp at the base. The actuators have silver paste on the contact pads to improve contact between the electrodes and the clamp. The actuator is clamped in a vertical position to avoid the influence of gravity. The resultant deflection of the actuator is measured using a laser distance sensor aimed at the tip of the cantilever, which is sent into the data acquisition device along with the input signal from the function generator and recorded using programs in LabVIEW. This allows the input voltage and deflection signals to be recorded simultaneously and compared. The actuator, clamp, and laser distance sensor are all contained inside an acrylic chamber to isolate the system from external disturbances or airflow and keep all electrical contacts

isolated for safety purposes. The transparent cover is connected to the voltage amplifier; once it is lifted, the amplifier will go into a limit mode to protect users and devices. The displacement measurement was done with the wrinkled single layer DEA (A2). The sample was excited with 40V, 80V, 120V, 160V, 200V, 240V, 280V, 320V, and 360V amplitude sinusoidal wave signals to visualize the actuation behavior better. The prototype DEA is long-term reliable up to 320V. The intended measurement is the displacement response from the actuator to the sinusoidal excitation in the time domain and extracting the Bode plots from the measurement data. Based on the displacement data, a hysteresis plot of the tested DEA can also be drawn, which will be further discussed.

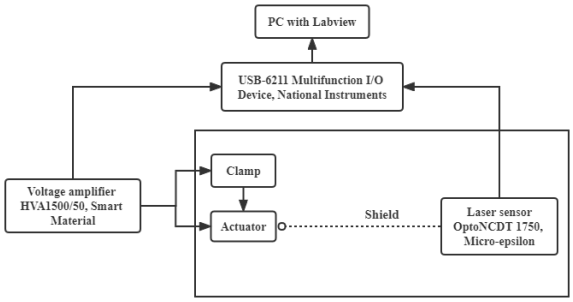

Figure 2.7. Measurement setup diagram for characterizing actuators.

3

Results

3.1. Manufacturing results of actuators

This section will tell the manufacturing results. All samples were manufactured according to the methodology in Section 2.2.4, and measurements were taken using the setup described in Section 2.3.1. The completed actuators, as well as the intermediate steps of manufacture, are shown in Figure 2.5. The actuators were manufactured in the form of cantilever beams with dimensions of 2.5mm×14mm, where 3.5mm×18mm is covered by PDMS. In the following subsections, results from each layer fabrication will be described from bottom to top of the actuators.

3.1.1. Bottom electrode

In the fabrication process of the bottom electrode, only one nozzle of the print head was activated for printing. Even though using more nozzles can save printing time, it could lead to lousy surface quality, especially causing gaps/voids on the silver track. This is not expected since the goal is to print a complete, smooth, and conductive bottom silver electrode. In addition, droplets fall in parallel when using several nozzles, and the droplet trajectory is misaligned, leading to blank space on the electrodes. Thus, the minor goal of having bottom electrodes with smooth and complete surfaces was reached with a nozzle to print. As seen from Figure3.1(a), the surface of the bottom silver electrode was continuous, with overlaps of each droplet spot. However, the surface continuity using three nozzles to print was worse than using one nozzle. The obvious blank space (dark stripes) under the bright stripes was shown in Figure3.1(b).

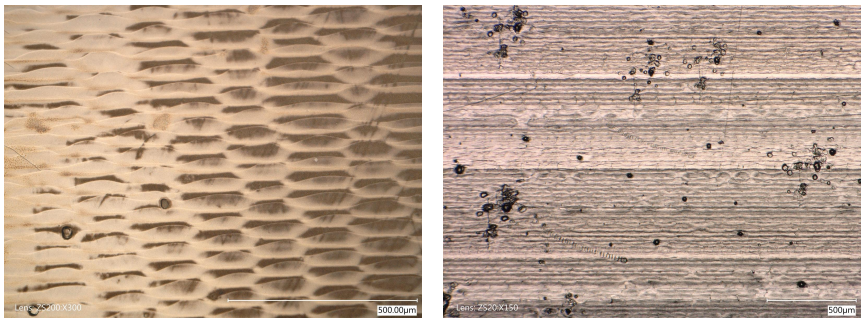

(a) (b)

Figure 3.1. Surface morphology of the bottom electrodes printing with one and three nozzles. (a) The bottom electrode printed with one nozzle. (b) The bottom electrode printed with three nozzles printing.

3.1.2. Printing of Dielectric elastomer layer

In the fabrication process of the DE layer, four different PDMS solutions were prepared and printed at 20%, 25%, 33%, and 50%, respectively. The concentration ratio depends on literature and experiments, where details are in section 4.1. The printing process follows the steps mentioned in subsection 2.2.4. Silver tracks with different wideness, different substrate heating temperatures, and surface treatment times were applied to validate the inkjet printing of the PDMS solution. The success in printing PDMS(33%) will be discussed in this subsection, followed by the introduction of several failed attempts on the way to success.

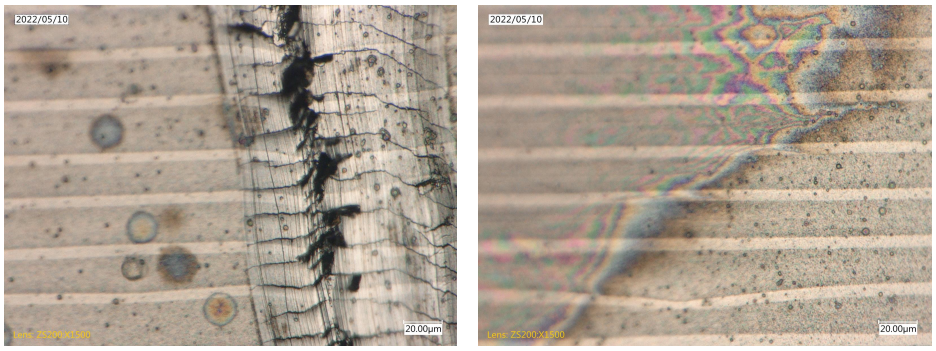

(a) (b)

Figure 3.2. Microscope observations of PDMS layer on the bottom silver electrode. (a) Focus on the PDMS defect. (b) The edge of the PDMS layer on the bottom silver layer, where the interference can be seen.

The most successful print of PDMS is applying the PDMS solution (ink) at 33% concentration. This PDMS solution was printed on the bottom electrode, with the substrate heating at 80°C. The print was performed twice, ending up with 2 layers of printing PDMS. The first layer would be semi-cured during printing due to the high temperature of the substrate table, leading to better adhesion of the second layer of PDMS.

To check if the printed PDMS(33%) layer can fully cover the bottom electrode, minor defects were made randomly on the PDMS layer by using a sharp tool to scratch, as shown in Figure 3.2(a). The criterion is: that if the scratch did not damage the bottom electrode, the PDMS could be said to cover that part of the bottom silver layer. To further prove the coverage, the edge of the PDMS layer on the bottom electrode was observed under the microscope, as shown in Figure 3.2(b). Again, interference can be seen on the edge of the PDMS layer due to the height difference of layers and the different reflective coefficients of the two materials.

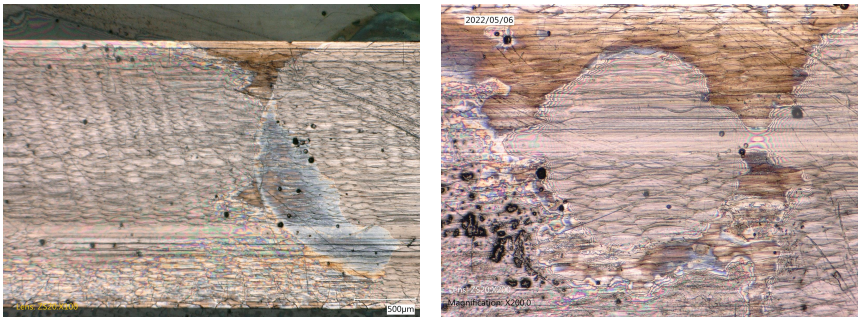

(a) (b)

Figure 3.3. Top view of the nonfully covered bottom electrode with printed PDMS at a concentration of 20%. (a) Full view of the 8 printed PDMS layers on the bottom electrode after oxygen plasma treatment. (b) Enlarged view of the printed PDMS layer on the bottom electrode after the oxygen plasma treatment.

Figure 3.3(a) shows the result of the attempt to print PDMS solution (20%) on a bottom silver electrode. The substrate was heated up at 45°C, and the sample was not cured to let the PDMS flow evenly. However, PDMS droplets cannot be fully covered, or they did not cure on the bottom silver electrode even though the sample was left to rest for a day after printing. A Close-up of the non-covered part is shown in Figure 3.3(b), where the darker part is the bottom electrode, and the brighter component is the PDMS layer. There is apparent dark space in the middle of the brighter part, showing the non-fully covered phenomena.

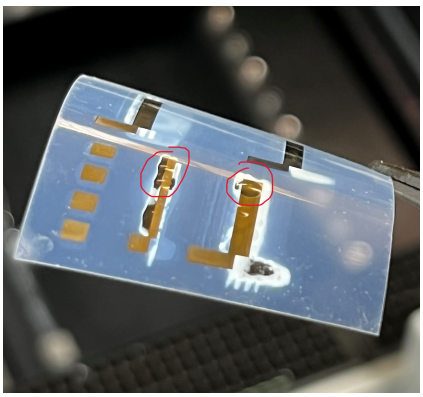

Figure 3.4. Printed PDMS(50%) on the thin and wide silver tracks, forming huge droplets.

Later on, thin and wide silver tracks were prepared, and new tries of PDMS(50%) printing(no-curing) were operated. The reason for preparing two silver electrodes of different sizes is to see whether the wideness affects the coverage of PDMS on the silver surface. Besides, a high concentration of PDMS solution enlarges the viscosity and helps PDMS stay on the silver surface after printing and before curing. In the Figure 3.4, several clear huge drops are shown and outlined by red circles. The drops cover most of the thin track while leaving the edge of the wide track uncovered, presenting that printing on the thin track can prevent missed coverage on the bottom electrode compared to wide tracks. However, 50% concentration PDMS solution is too viscous for printing since the printing drops were not stable and too viscous to form a flat polymer surface.

3.1.3. Surface treatment and Thickness measurement of DE layer

A repeated treatment cycle is the most suitable surface treatment process to achieve a hydrophilic PDMS surface for top electrode adhesion. Each treatment round is operated for 6s, and a break is inserted between two treatments. The total treatment time will be 42s, summing up 7 rounds. The optimized oxygen plasma treatment cycle for the PDMS layer was adopted based on literature and experiments, which will be discussed in section 4.1. The non-wrinkled result can be seen in Figure 3.5(b). The PDMS layers were smooth and flat compared with the rough/wrinkled PDMS edge shown in Figure 3.5(a). The wrinkle issue was solved by applying different surface treatment processes. Therefore, an inkjet-printed PDMS layer was successfully obtained. The wrinkles on edge can be minimized by curing the PDMS for a longer time(>2h) before applying oxygen plasma treatment.
On the way to gaining insights for a suitable treatment time, the inkjet-printed PDMS layer was continuously oxygen plasma-treated for 1min and surface checked. However, as can be seen from Figure 3.6(a) and 3.6(b), many wrinkles appeared after oxygen plasma treatment, which was 1min long. The wrinkles appeared from the middle to the edge, distributing over the entire PDMS layer.
Lastly, to measure the thickness of the printed PDMS layer, a DEA sample was cut and observed under SEM. This type of imaging requires the sample to be conductive. A non-conductive sample will build up a static surface charge when imaged with an electron beam [28]. It is the barrier to observing samples in clear view since the charged surface will lead to overexposure. The surface to be observed should be conductive in two ways: coated with gold particles or connecting the metal stage with conductive tape. A sample cross-section is required to observe the PDMS layer thickness with cutting by a femtosecond

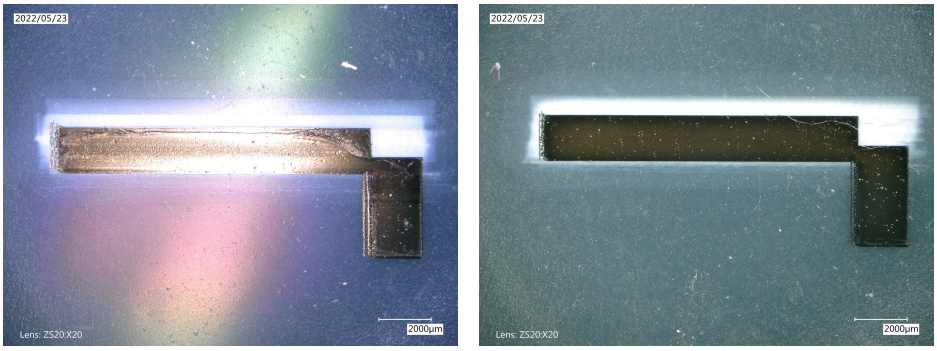

(a) (b)

Figure 3.5. Observations for samples with bottom electrodes and PDMS layers, by Keyence. (a) The sample with wrinkles on the PDMS edge after another optimized oxygen plasma treatment(18s +18s+12s). (b) The sample with no wrinkles on PDMS after the optimized oxygen plasma treatment(6s×7).

laser cutting device. The thickness of the printed PDMS layer (upper part in the figure) is roughly 29µm, as shown in Figure 3.7(b).

(a) (b)

Figure 3.6. Observations under microscope for the wrinkled PDMS and close-up of wrinkles. (a) The inkjet printed PDMS layer full of wrinkles after 1min oxygen plasma treatment. (b) Close-up of the wrinkles on the PDMS.

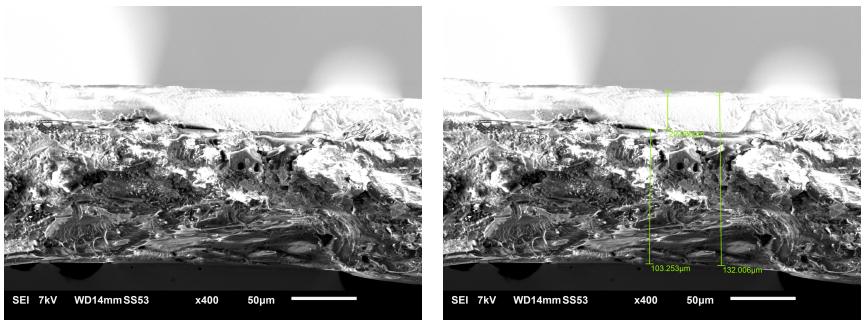

(a) (b)

Figure 3.7. Thickness measurement for PDMS layer, by SEM. (a) Cross-section of the PDMS layer on the bottom electrode and the PET substrate. (b) Cross-section of the PDMS layer with dimensions.

3.1.4. Top electrode

This subsection will first include the successful fabrication of the conductive top electrode printing, then goes into the attempts to achieve success. Top electrodes were printed on PDMS layers following the

steps mentioned in subsection 2.2.4. The conductive top electrode without cracks was achieved in conditions:

- The polymer layer was fully dried out and cured for at least 2h as mentioned in subsection 2.2.4. (No solvent left on the polymer)
- The polymer layer was oxygen plasma-treated just before printing. (better less than 2h)
- No wrinkles on the polymer layer.
- The curing and sintering time for top electrodes were precisely controlled as mentioned in subsection 2.2.4.

Successful printing of the top electrode is shown in Figure 3.8(a). Even though the top electrode is conductive, it has minor cracks across the entire surface. A close-up of the cracks is shown in Figure 3.8(b). The top electrode resistance is about 7Ω, measuring from the tip to the bottom. However, this work is not repeatable, so a more reproducible manufacturing method/process remains to be operated. The discussion about it is on section 4.1.

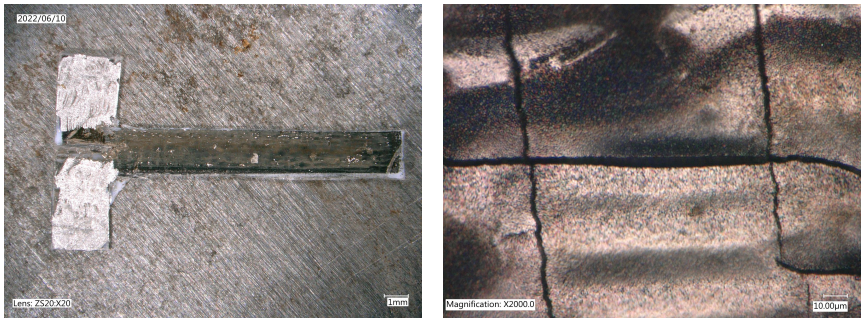

(a) (b)

Figure 3.8. The surface observation of a conductive top electrode. (a) The overview of a conductive top electrode. The single layer DEA (A1) having a top electrode without huge cracks. (b) Close up of the cracks on a conductive top electrode surface.

Some observations were made to study this challenge and figure out a reproducible method. First, an overlook of a cracked top electrode on the wrinkled PDMS layer is shown in Figure 3.9(a). In this case, only one layer of the top electrode was printed on the PDMS layer. The middle part of the electrode has bad surface quality, with voids and cracks. The vast cracks distributed over the silver top electrode surface would badly affect the conductivity.
Figure 3.9(b) shows an actuator with cracking on the surface. The silver electrode was printed one layer on the oxygen plasma-treated PDMS surface (no wrinkles). The middle part of the thin layer of the electrode is off from the polymer surface. The enlarged view of the cracking area is shown in Figure 3.9(c). The peeling-off phenomena in the middle of the electrode are clearly shown in it, and the bottom electrode is visible through the hole on the top electrode and the transparent polymer layer. The edge of the top electrode is of good morphological quality, being smooth and continuous. Compared to the sample shown in Figure 3.9(a), the cracks here are more significant even though the area without cracking is smooth and shiny.
To solve the floating problem, a printing test was done with a PDMS cover on top of the top electrode. The morphology result of this trial is shown in Figure3.10(a). The top electrode was only printed once and covered by 2 layers of printed PDMS. Compared with the previous peeling-off result, the electrode does not flow off from the polymer this time, thanks to the top PDMS layer. However, due to the tendency to flow, many wrinkles appeared on the top electrode. Those are not solved by printing top PDMS film. The close-up of the wrinkles can be seen in Figure3.10(b). Besides depositing a printed PDMS layer on top, a spin coating PDMS layer was deposited on a top electrode. However, not only

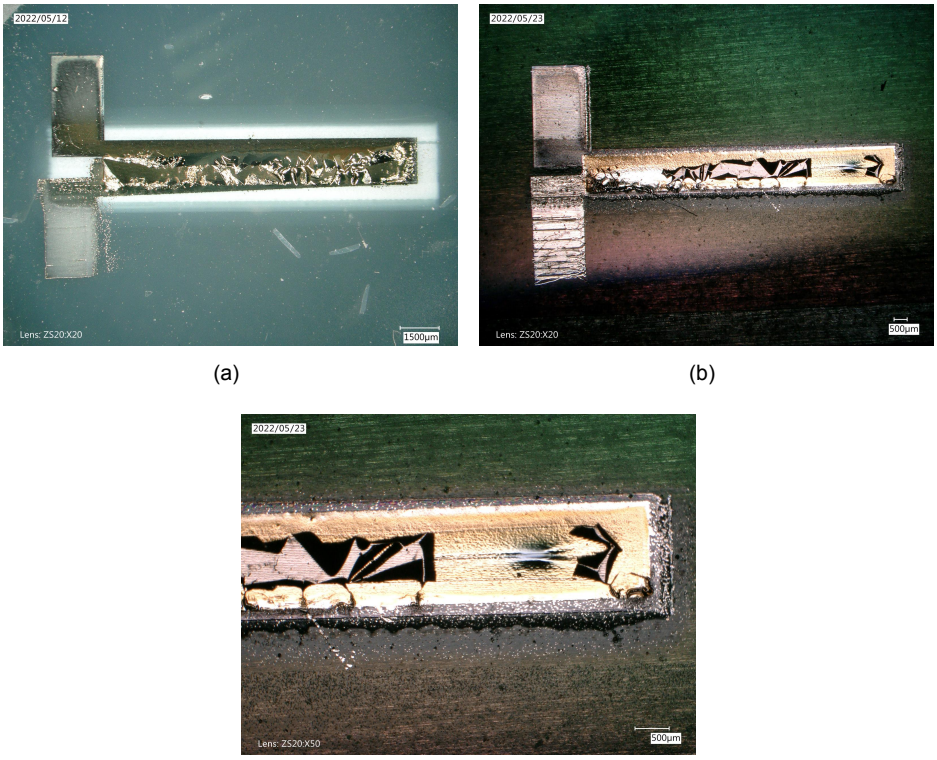

Figure 3.9. Observations for failed DEAs on the surface defects. (a) Full view of cracks on top silver electrode on wrinkled PDMS layer. (b) Full view of a single layer DEA with the cracked top electrode. (c) Close-up of the cracking space on the top electrode.

wrinkles appear in this sample, but also the loss of part of the top electrode due to the centrifugal force in the spin coating process.

In an attempt to solve cracking, an extra silver layer (using MU01 silver ink) was printed on the top electrode. It was intended to fill the cracks. Results are displayed in the Figure3.11(a) and 3.11(b). However, the extra silver layer did not fill the cracks as expected. The produced droplets in printing this extra silver layer stayed separated on the surface of the top electrode, which is shown on the right of Figure3.11(b). The silver surface remained cracked and non-conductive.

The subsequent filling method was applied to again fill the cracks on the printed top electrode, applying the JS-A211 silver ink in printing the top electrode and repeating the printing three times. The repetition ensures the filling succeeds, forming an entire surface of the top electrode. As shown in 3.11(c) and compared with Figure 3.11(a), some cracks are filled while the rest remain. The close-up in Figure 3.11(d) shows a smooth part on the top electrode, where cracks were filled. The resistance of the top electrode is still relatively high, at 2MΩ; therefore, this top electrode is not conducive.

3.1.5. Actuator results

In order to achieve functional actuators in the end, every manufacturing step should be carefully and strictly operated to gain ”perfect” layers. Only with ”perfect” layers can functional actuators be obtained. They require conductive electrodes without major cracks (top and bottom), and a hydrophilic dielectric elastomer layer entirely covers the bottom electrode. Figure 3.8(a) shows a single layer DEA, with a cracked and conductive top electrode and silver paste for better electrical connection. Another functional single layer DEA with a conductive top electrode is shown in Figure 3.12, with wrinkles on the top electrode. The top electrode is conductive and shows no significant cracks, and the DEA can be excited by the uni-polar input signal. The measurement results of this actuator will be discussed in

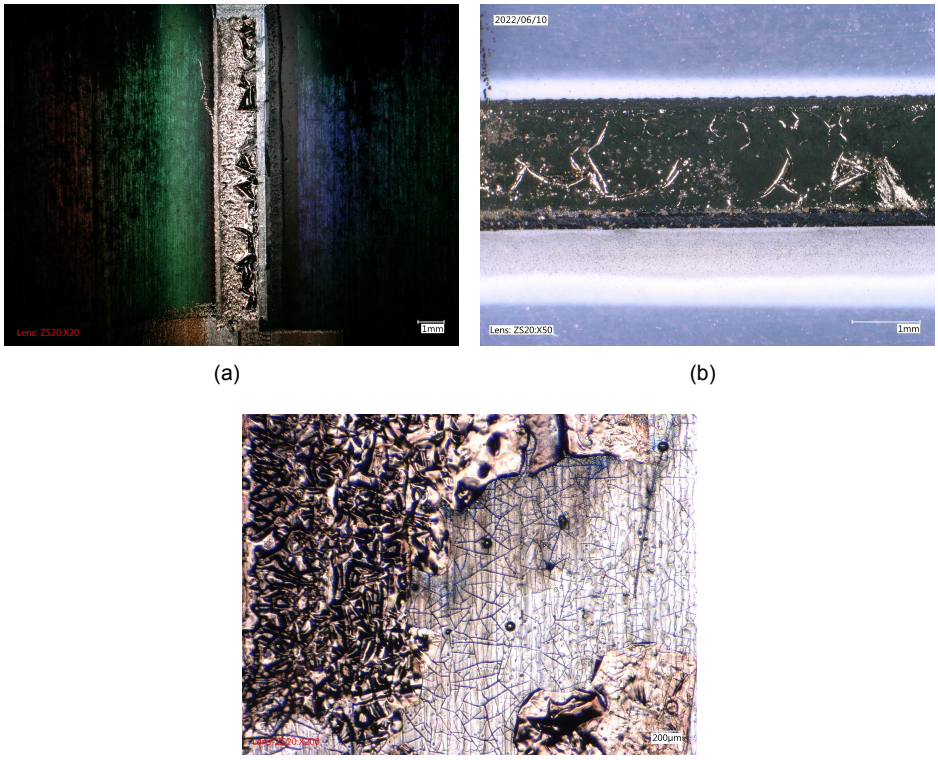

(a) (b)

(c)

Figure 3.10. Surface of top electrodes covered by PDMS layer on top. (a) The top electrode covered by printed PDMS on top. (b) Close up of top electrode surface with printed PDMS on top. (c) Close up of breakage on top electrode after coated with PDMS.

section 3.2. Further discussion about the DEA will be discussed in chapter 4.

Table 3.1: Resistance and Surface morphology of single layer DEAs

Sample	Resistance of top electrode / Ω	Surface continuity
A1	around 7	Smooth and continued
A2	around 200	Wrinkled but continued

3.2. Actuation characterization results

In this section, the actuation, hysteresis, and frequency response results of the DEA will be shown. Long-term usage with a voltage signal higher than 320V may cause contact pad failures and lead to non-conductivity. In order to have a consistent and comparable characterization of the DEA, a threshold voltage of 320V was followed. The steady-state deflection was achieved by driving with a 320V sinusoidal wave signal at about 3.21µm. The deflection of DEA reached 1.51µm when operated with a 320V sine wave signal at the resonance frequency.

The Figure 3.13 shows the deflection behavior of an inkjet-printed DEA when operated with sinusoidal voltage input signals (10Hz) with offsets. Figure 3.14 depicts the variation in deflection at the tip of the printed DEA in response to an excitation amplitude of up to 360V. The deflection vs voltage plots, as shown in Figure 3.15(a) and Figure 3.15(b), provide hysteresis loops, and the induced deflection has been fully regained and even a bit over during the unloading of the voltage input (10Hz and 5Hz). A plot depicting the measurement of the magnitude of deflection and phase of the actuator in response to the unipolar sinusoidal voltage with an amplitude of 320V input as a function of frequency is shown in Figure 3.16.

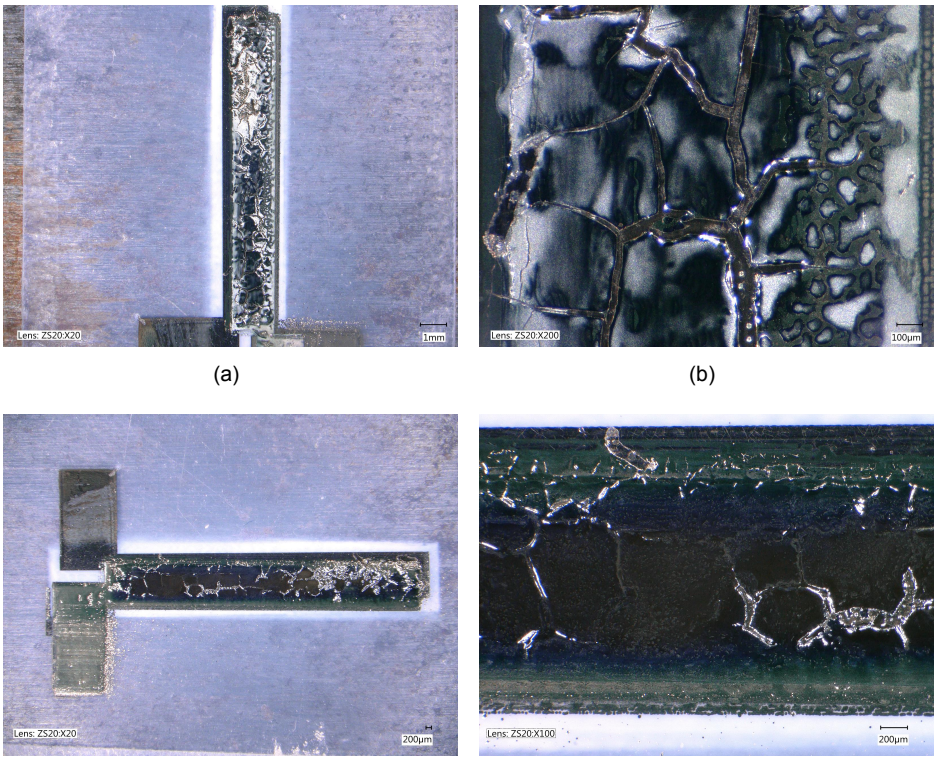

Figure 3.11. Surface morphology of top electrode covered by extra silver layers. (a) The top electrode (Sample F) covered by an extra silver layer on top. (b) Close up of top electrode surface with an extra silver layer on top. (c) The top electrode (Sample F) covered by four extra silver layers (one printed with MU01 silver ink, three printed with JS-A211 silver ink). (d) Close up of top electrode surface with extra silver layers on top.

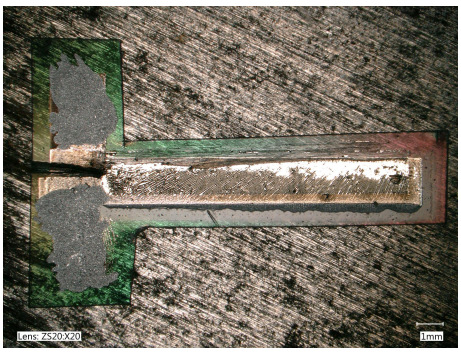

Figure 3.12. The single layer DEA (A2) having a top electrode with wrinkles but conductive.

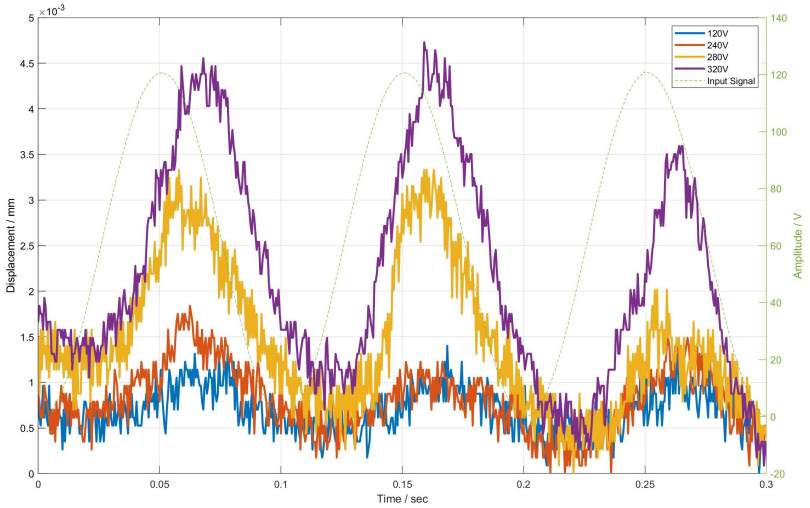

Figure 3.13. The plot of the deflection of the fully inkjet printed dielectric elastomer actuator when excited with sinusoidal wave input signals at 10Hz. This shows up somewhere in the middle of the drive and therefore shows the displacement ahead.

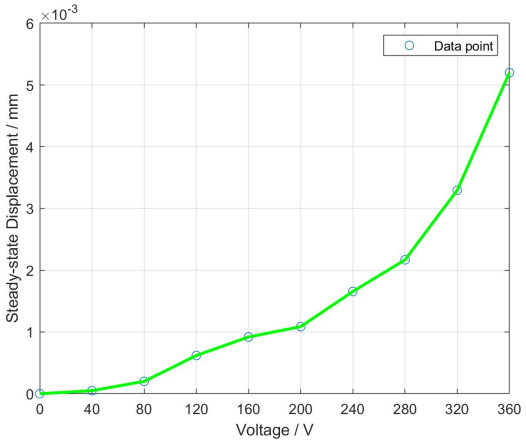

Figure 3.14. The plot of the steady-state deflection vs voltage (10Hz) of the fully inkjet printed dielectric elastomer actuator.

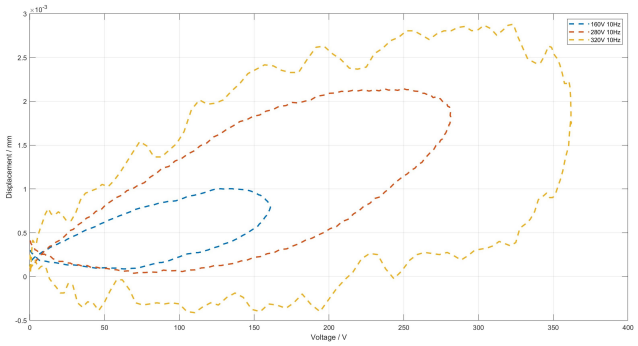

(a)

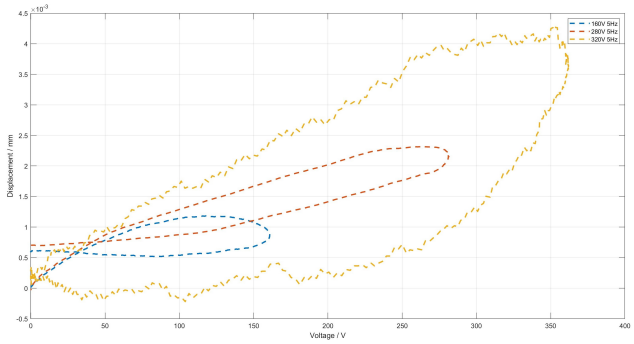

(b)

Figure 3.15. Hysteresis graphs of the DEA. (a) The hysteresis plot of the fully inkjet printed cantilever DEA employing sinusoidal wave input signals measured at 10Hz. (b) The hysteresis plot of the fully inkjet printed cantilever DEA employing sinusoidal wave input signals measured at 5Hz.

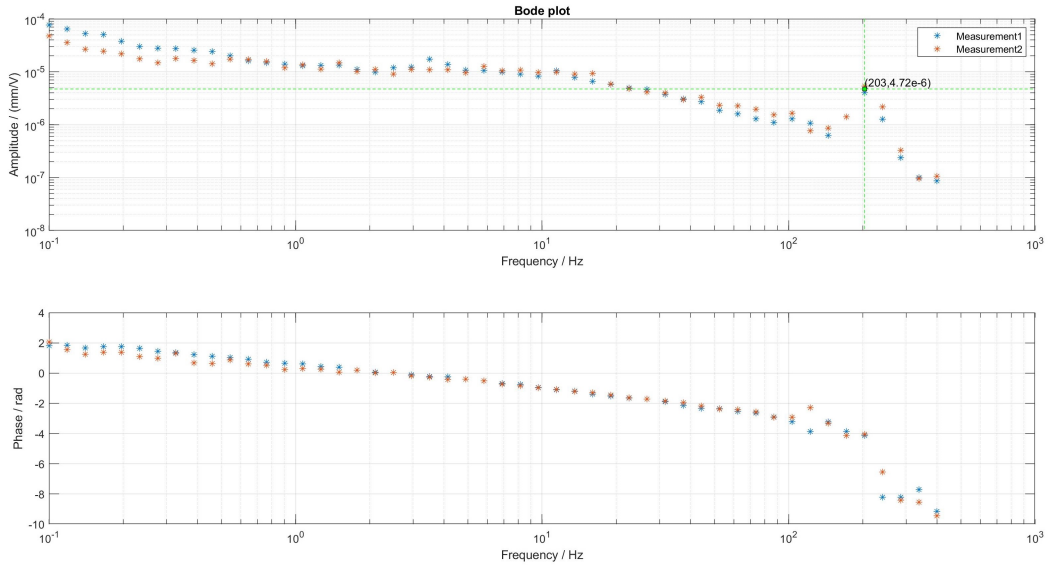

Figure 3.16. The bode plot of a fully inkjet printed DEA with measurement data points.

4

Discussion

4.1. Manufacturing

Table 4.1: The reasonable ranges for the physical properties of inks in inkjet printing.

Ink property	Reasonable range
Viscosity μ	0.008 Pa·s < μ < 0.025 Pa·s [29]
Particle size	< 10% nozzle diameter
Surface tension σ	0.020 N/m < σ < 0.035 N/m [29]
z-value (the inverse of the Ohnesorge number)	1 < z < 14 [30],[31]

The ratio of PDMS to solvent plays a significant role in affecting the physical properties of PDMS solution and further influencing printing. Therefore, in the work of Mikkonen *et al.* [32], they discussed, experimented with, and measured the viscosity and surface tension of PDMS-OA (octyl acetate) solutions at different ratios. The results also show several mixtures with different ratios of PMDS-OA, as results of viscosity versus temperature and surface tension can be seen in Figure 4.1(a) and (b), respectively. When the temperature is higher than 35°C, the PDMS solution at a 1:2 ratio will be printable since the viscosity is within the range for printing, while the PDMS solution at a 1:4 ratio is not. There is no significant difference in surface tension between the mixtures with a PDMS-OA ratio of 1:2, 1:3, and 1:4. Those three PDMS solutions are all accepted when only considering the surface tension value. In experiments, the print head temperature was controlled between 35°C to 50°C; thus, the viscosity of PDMS solutions is always within the printable range. Therefore, the PDMS solutions that were used to print in this work meet the basic printing requirements.

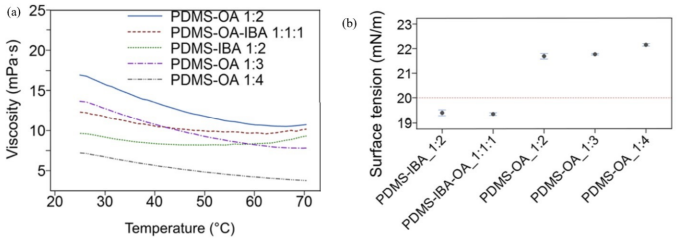

Figure 4.1. (a) Measured viscosities as a function of the temperature (25-70°C). (b) Measured surface tensions (15 measurements, confidence interval CI 95% for the mean) [32].

The wrinkles that appeared on the printed PDMS layer after oxygen plasma treatment are well accepted to be one of the mechanical instabilities. The surface wrinkling relieves the compressive stress

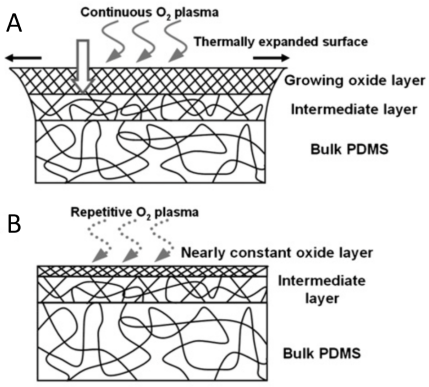

Figure 4.2. (a) Schematic representation of the PDMS system subjected to continuous plasma exposure. (b) Schematic representation of a PDMS system subjected to repetitive short-period plasma exposures. Edited from [33].

for minimizing the systematic free energy, often produced from the strain mismatch between a stiff skin and the underlying compliant foundation. In some studies on PDMS wrinkling, thermally heated and pre-strained PDMS underwent surface oxidation and finally generated compressive stress for wrinkling upon cooling process [33]. As shown in Figure 4.2A, due to the temperature rise in the bulk gas, the surface oxide layer thermally expands, and its thickness increases with the duration of plasma exposure. For the sample that underwent a repetitive treatment, the thermal expansion of the surface oxide is firmly eliminated, and oxygen penetration is limited due to temperature quenching, as Figure 4.2b shows. In the case that the electrodes printed on the wrinkled PDMS, the defects would be caused by the wrinkles, which prohibit a continuous deposition of the silver layer as shown in Figure 3.9(a). In experiments, first, a treatment cycle with 3 rounds (18s+18s+12s) was adopted; however, the results still showed wrinkles on the surface. With the advice from the literature and supervisor, another treatment cycle was operated with 7 rounds, and each round lasted 6s. This treatment provided decent results in reducing wrinkles on the PDMS surface.

When discussing the top surface cracks that appeared after ink curing, Kang *et al.* [34] proposed the reasons: one is not having enough material; the other has too much material, causing cracks to grow. In this inkjet printing electrode, the latter reason seems more acceptable. Comparing the results from one layer electrode Figure 3.9(c) and multi-layer electrode Figure 3.11(a) and Figure 3.11(c), we can see more smaller cracks (not peeling off) on the multi-layer electrode. Some minor cracks might appear when the printed top electrode is drying. Therefore, when the material accumulates too much, the thickness of the top electrode will exceed the critical thickness, leading to the growth of cracks. Therefore, having one/two-layer top electrodes is a better solution for fabricating the inkjet-printed silver electrodes than having more than 3 layers. Besides, the JS-A211 silver ink owns a high load factor at 40%, which can also lead to unexpectedly fast material accumulation. Therefore, examining top silver ink printing on PDMS layer will be the main work for having conductive and complete top electrodes in future work. Besides, air humidity might also affect solvent evaporation; the successful fabrication of the actuator was made on the 23th May, a sunny day, while the reproduction was operated on the 8-10th of June when it rained all the time. Thus, solving the problem of the non-reproducible printing process will provide an opportunity for fabricating the stacked DEAs in the future.

4.2. Characterization

From Figure 3.13, the deflection of the printed actuator was able to follow the trend of the sine wave, going up with voltage rising and going down when the voltage dropped. However, a response delay can be seen in the time shift from the displacement curves to the input signal. The phase lag in the displacement response is about 0.35π. Besides, the actuator tended to move further away from the sensor, as the position value at the valley was lower than before being actuated, as shown in Figure 3.13. The sine

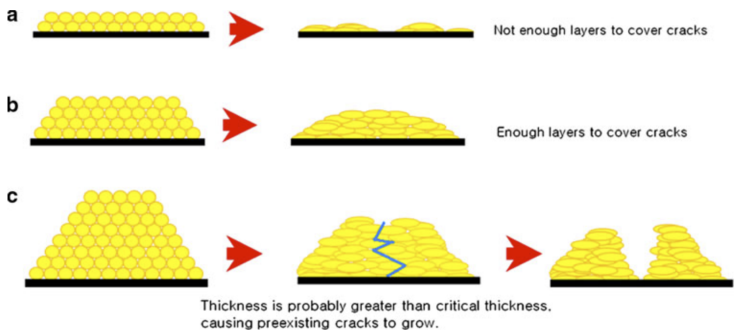

Figure 4.3. Schematic drawing of a producing preexisting cracks [34].

deflection of cantilever DEA is solely due to the property of electrostatic force, while the displacement shift may be due to the power loss and heat dissipation. Due to such small deflections, the longitudinal displacement approximately equals the contraction deformation. Thus, the radius of curvature R of the dielectric elastomer unimorph is inversely proportional to the longitudinal strain, such that

$$\frac{1}{R} \propto s_z \propto V^2 \tag{4.1}$$

This derives that the curvature is inversely proportional to the square of the driving voltage. The theoretical trend of curvature agrees well with the experimentally measured one as shown in Figure 3.14. From Figure 3.15(a) and 3.15(a), the hysteresis displacement curves show different rising and dropping performances, having concave and convex curves, respectively. The phase lag on the displacement response to the input signal can also be confirmed in the hysteresis plot, with the maximum displacement mislocating the maximum voltage. In addition, the larger the input signal is, the more significant displacement can be achieved with more considerable hysteresis. When analyzing the frequency response, applying input signal at a lower frequency leads to higher steady-state displacement, which can also be witnessed at the decreasing tendency of the gain margin in Figure 3.16. The resonance frequency of the full inkjet printed DEA with PDMS layer was determined to be 203Hz, as seen from the frequency on the peaks in Figure 3.16.
Further research could be dealt with a more reliable printing process for the top electrodes and the fabrication of a fully inkjet-printed multilayered/stacked actuator which could enhance the deflection capabilities of a cantilever with similar or even smaller voltage inputs. Finding a more suitable printing and treatment method for top electrodes to be printed on the PDMS layer could be one of the leading research goals in the future. It can require maintaining specific conductivity, achieving a complete electrode surface, and gaining few defects.

5

Conclusion

This thesis proves the viability of an fully inkjet-printed dielectric elastomer actuator fabricated with silver inks and PDMS solution. The cantilever DEA in this work comprises an intermediate layer of a dielectric polymer PDMS between the Ag electrodes and is fully inkjet printed onto a coated substrate. It opens the way for inkjet-printed DEAs with performance and ease of manufacture not previously possible. The manufacturing process and measurement of actuators demonstrate fabrication problems, solutions, and outcomes. In order to achieve this, an introduction was first given to form a foundation as to what is the application of DEAs, problems with existing products, what fabrication methods DEAs exist, and what efforts have been made to produce DEAs, and the research goal. Following this, structures, working principles, and designs were presented, giving an overview of what will be fabricated and the rules to follow. It provides the necessary basis for constructing the actuator, manufacturing process, and measurement setup.

The challenging part of the manufacturing process was the printing, curing, and treating of the dielectric polymer layer and the top electrode. The results chapter gives the manufacturing and measurement results of each layer in the fabrication process, comparing the printing results from different (treatment) methods. A manufacturing process flow consisting of inkjet printing of the polymer (PDMS) layer and polymer surface treatment was adopted to achieve a functional actuator. The inkjet-printed PDMS layer can be achieved by printing a 33% concentrated self-prepared PDMS solution on top of a heated (80°C) substrate table in the printer, having a thickness roughly at 29µm. However, the PDMS surface presents hydrophobic performance after curing, preventing stable adhesion of films on it. With the optimized oxygen plasma treatment cycle, which requires 7 rounds of treatment with 30s breaks between each round, the inkjet-printed PDMS surface can perform no wrinkles and hydrophilicity. These allow the latter top electrode printing and ensure the completeness of the top electrode surface. The top electrode printing, however, is not consistently repeatable. Even though two conductive top electrodes were fabricated with low resistance (7Ω and 200Ω) and showed minor surface defects which do not affect the conductivity, most of the top electrodes in DEAs still have cracks and high resistance. It tells that the manufacturing method or the silver ink for the top electrode is not ideal and could not lead to a high success rate. New treatments to get complete and defectless electrodes were operated on even though unsuccessful. The fully functional cantilever DEA provided a stable deflection of 3.21µm at 320V and can be operated up to 203Hz. The displacement at resonance is 1.51µm, and the phase lag/ response delay is about 0.35π.

The current study demonstrates the ability of an additive manufacturing technique to fabricate a functional DEA. However, the DEA does not work perfectly, having a more negligible deflection than the theoretical value due to the imperfections of the top electrode. The gap in the literature on inkjet printing smooth and complete polymer(PDMS) and silver layers and realizing a fully inkjet-printed cantilever dielectric elastomer actuator is accomplished but with future challenges. With interest in enlarging the

stroke of DEA, the fully inkjet-printed multilayer/stacked DEA will be the next goal.

6

Recommendations

The deflection and frequency response results achieved by the actuators show acceptable results, indicating an improvement over what has been achieved in the literature. However, there remains potential for further research in the inkjet printed DEAs, with several areas that can be improved. This chapter will give recommendations/tips on ink preparation, fabrication related, and future research.

PDMS solution

- The ratio between the curing agent and the PDMS can be examined. A lower ratio can provide better flexibility for the PDMS film.
- Be careful about the humidity in the air and also the ages of the self-prepared PDMS solutions. Further work should investigate if these same PDMS solutions allow good adhesion performance of the top electrode in different weather.
- Different diluting solvents can be examined to further determine the possibility of being printed on the top electrodes. This could be helpful in researching the multi-layer DEA.
- Due to the curing property of the PDMS solution, a clever way to clean up the print head should be risen. This could save some time in the lab.
- Different concentrations of PDMS solutions and different numbers of printing layers could be investigated, which might give a thinner PDMS layer and, thus, better displacement and frequency response results.

Top electrode

- A more sustainable fabrication method for printing the top electrode should be investigated. Further research might be related this to the multi-layer DEA fabrication.
- The size/shape of the DEA could be optimized/enlarged to further avoid unexpected breakdowns on the contact pads during actuation. It could also be effective in adapting different applications.

Cartridge related

- Better quality cartridges might be used in the future, providing more stable storage of the silver NP inks.
- Cartridges should be stored in a fridge when they are not used, reducing the possibility of clogging the print head.

A

Printing setting details

KONICA MINOLTA 512 print head settings

Droplet shape and velocity

In order to have a stably jetting behavior, droplet velocity should be within a specific range, which is about 4m/s to 6m/s. Besides, the satellite shapes should be avoided, and the timing of the waveform matters, as shown in Figure A.1. The shape and velocity of the droplet can not only be controlled by the amplitude of voltage but also the timing.

DMC 16110 print head settings

Print speed, DPI (dot per inch) resolution and frequency

Due to the principle of not damaging the machine, the printing frequency is ideally no more significant than 1kHz. A lower print speed generally produces better quality prints but increases print time. On the other hand, a higher jetting frequency allows for faster printing. However, low viscosity inks usually perform better at lower frequencies. The print resolution is based on the drop size and drops spacing on the substrate in combination with the desired definition of the print. Therefore, the printing speed for each ink/figure can be calculated with the integrated DPI calculation module inside the software.

Substrate table

The substrate table supports the sample. It has several small holes which can suck the substrate. Besides, it can be heated up to 90°C, which is suitable for thermal curing. However, the substrate table can only move in the Y direction and rotate around the Z-axis.

Print direction

The default printing direction setting is in Y uni-direction, which is along the trail of the substrate table. In this study, the printing figures are long in the Y direction; therefore, printing in the Y direction reduces the number of printing paths and saves printing time. Besides, the uni-directional printing can help with the droplet alignment and has well repetition.

Print head temperature

In PIXDRO LP50, a print head heating module is typically used to heat the print head. With high print head temperature, the droplet velocity will increase. However, it is unacceptable that the print head temperature goes too high since it will cause unpredictable bad results. Especially with long continuous prints, the print head temperature will rise even though the heating module is off. It will cause the ink properties to change, such as the viscosity, influencing the jetting behavior. If the print head temperature is fixed at a specific value, going out of this range can cause an error and stop the

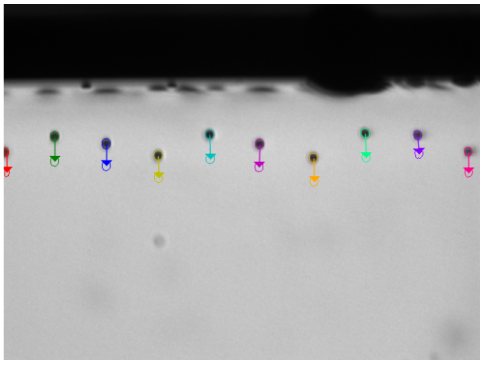

	v (m/s)	V (pl)	X (µm)	Y (µm)	Angle (°)
→	1.88	± 1.6	8	420	1.11°
→	2.33	± 8.5	145	376	0.24°
→	2.07	± 8.6	292	396	0.14°
→	2.06	± 8.7	440	430	0.96°
→	2.28	± 8.3	586	370	1.22°
→	2.15	± 8.3	728	397	-1.31°
→	2.22	± 7.7	881	436	1.51°
→	2.26	± 7.7	1029	366	2.42°
→	1.75	± 7.0	1178	372	3.77°

(a) (b)

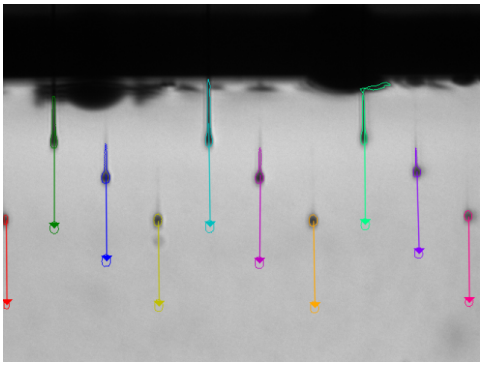

	v (m/s)	V (pl)	X (µm)	Y (µm)	Angle (°)
→	7.94	± 2.0	8	612	0.54°
→	9.20	± 13.8	144	359	0.22°
→	8.14	± 11.8	292	483	0.26°
→	8.04	± 9.4	440	613	0.58°
→	9.79	± 15.5	585	337	0.55°
→	8.29	± 11.1	730	484	-0.32°
→	8.18	± 9.4	881	614	0.85°
→	10.88	± 28.8	1027	298	0.44°

(c) (d)

Figure A.1. Data of controlling the velocity and path of droplets from the KM512 print head. (a) Dropview (KM512 print head) with 14V upper voltage, 7V lower voltage, 3µs ON Pulse time, and 3µs OFF Pulse time. (b) Velocity, volumn, and path of droplets. The data within the red frame is considered relatively accurate. (c) KM512 print head with 14V upper voltage, 7V lower voltage,4µs ON Pulse time, and 3µs OFF Pulse time. Testing with blue ink. (d) Velocity, volumn, and path of droplets. The data within the red frame is considered relatively accurate.

Table A.1: Printing settings for Mitsubishi NBSIJ-MU01/ Novacentrix JS-A211 silver inks

Parameters	Value and unit	Parameters	Value and unit
Up down	9.0μs	End Ramp	5.0μs
Indle Before	6.0μs	Idle After	7.0μs
Fill Ramp	5.0μs	Substrate Heating	35°C / 45°C
Time Low	6.0μs	Head Heating	28°C
Fire Ramp	1.5μs	Ink Pressure	-5mbar
Time High	7.0μs	No. of print repeat	2 / 1
Frequency	950Hz		

print. If the temperature in the print head rises high enough to evaporate the solvent, the nozzles can clog (partially), and the printing will be ruined. The printer has no cooling module; thus, there is no possibility of cooling down the print head if the temperature goes too high. The print head DMC-11610, Fujifilm Dimatix, can be heated up to 60°C.[35]

Nozzle

The number of nozzles is constrained by the print head that is used. For example, the DMC-11610 print head, Fujifilm Dimatix[35], can provide a 10pL droplet each time. The nozzles are 20μm in diameter; each can jet a droplet in 10pL volume per shot. The pitch is 254μm, and there are 16 nozzles in the print head. However, in reality, it is possible that not all the nozzles are working, which is highly related to the printing voltage applied.

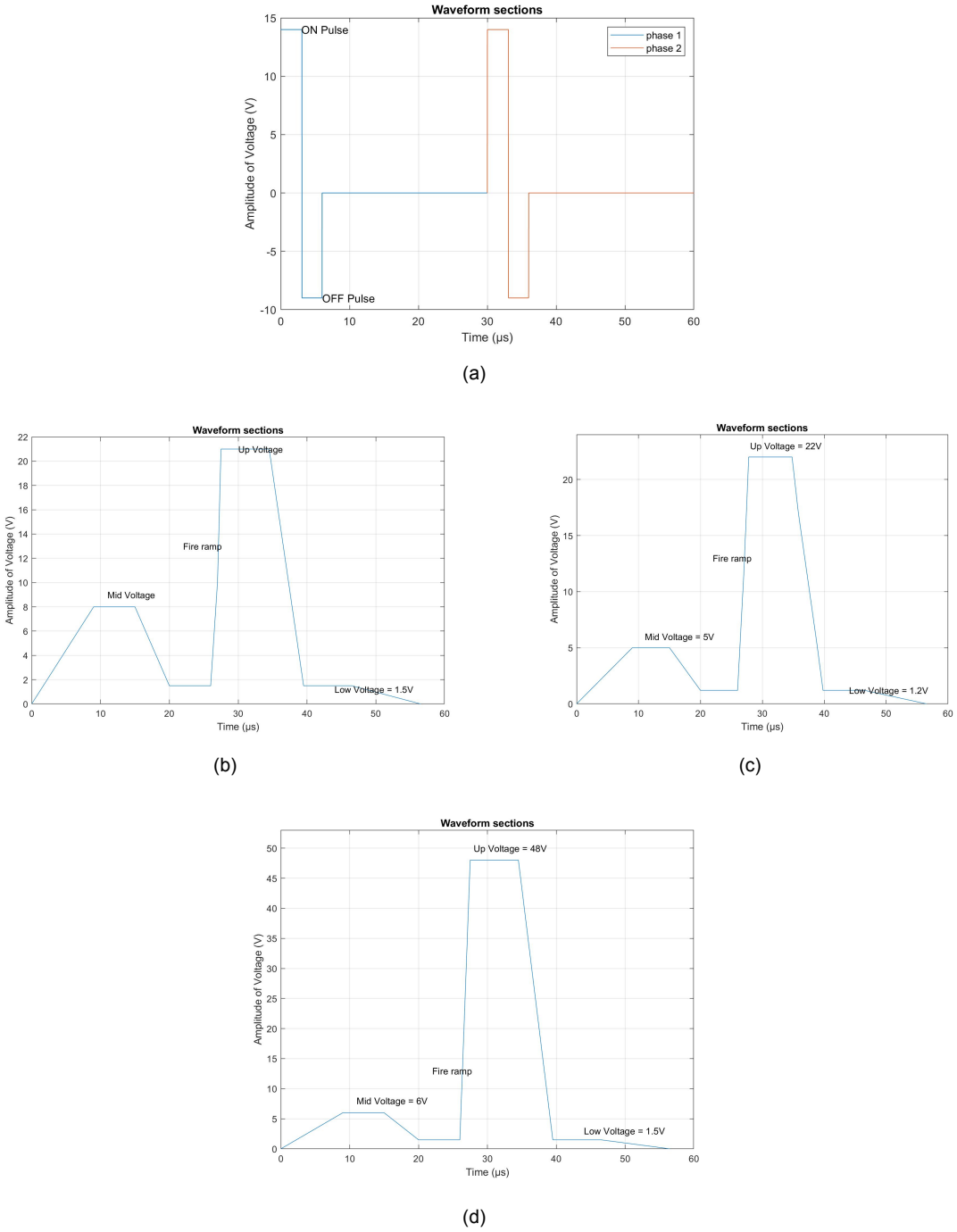

Figure A.2. Waveform of different inkjet printed inks using different cartridges. (a) General waveform for KM512 print head. (b) Waveform for the Mistubishi NBSIJ-MU01 silver ink using the DMC cartridge. (c) Waveform for the Novacentrix JS-A211 silver ink using the DMC cartridge. (d) Waveform for the self-prepared PDMS(33%) ink using the DMC cartridge.

B

Manufacturing

The defects on the bottom electrode were observed under the white light interference microscope. Greenlight was used to brighten up the view because it is less bright than white light, allowing a clear picture of the reflecting surface and also the transparent surface. This is observed with a 50 times magnification objective. Small dust and leading cracks on the top silver surface were observed. The height of the dust is about 5 μm, which is quite reasonable, for two layers of the bottom electrode is about 1.5 -2 μm thick.

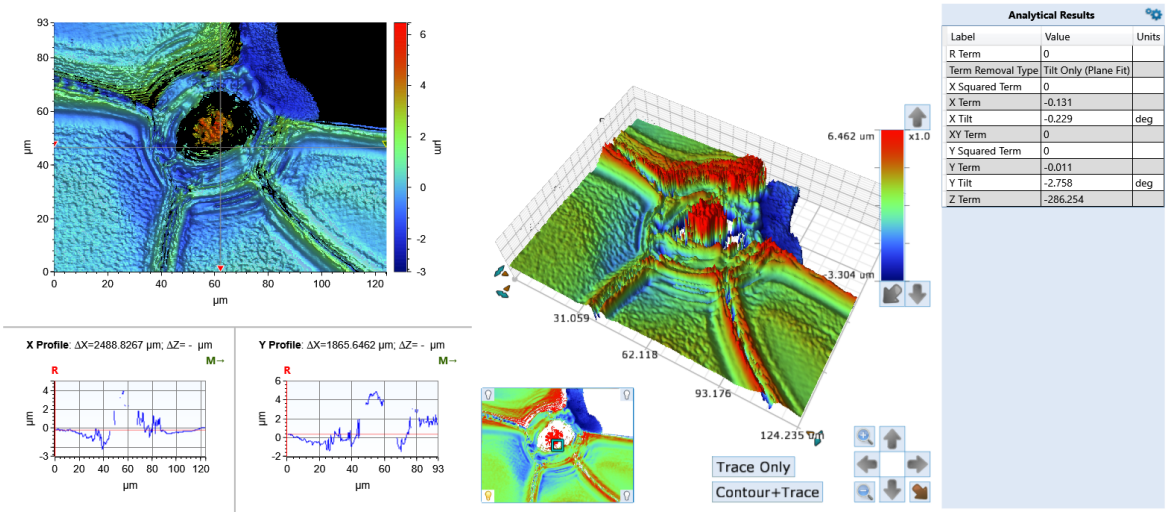

Figure B.1. The 3D profile of defects on the bottom electrode.

Here below shows some failures/defects in DEAs that affect the conductivity and surface smoothness. Figure B.2 show different types of defects and the surface morphology of several DEAs.

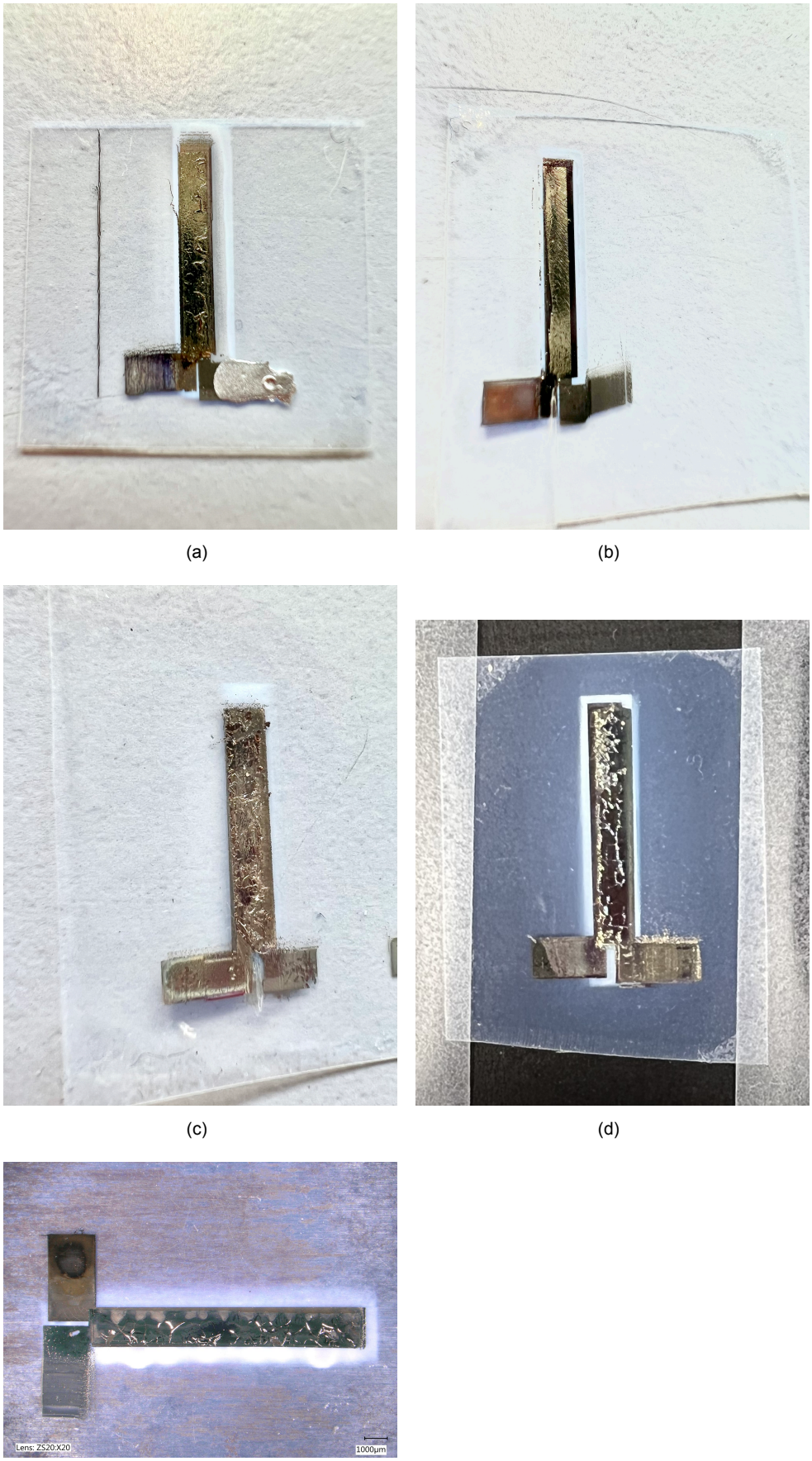

Figure B.2. Several DEAs with different types of failure/defects. (a) A single layer DEA covered by a top PDMS layer. The sample has electrode wrinkles and cracks caused by the deposited PDMS cover. No short circuit between the bottom and top electrodes presents. (b) A single layer DEA with relatively complete and smooth top electrode surface. No short circuit shows, but wrinkles appear on the surface. (c) A single layer DEA with failures, including short circuit, and cracks. However, it is partially conductive on the top electrode. (d) A single layer DEA with failures, including cracks and non-conductivity. (e) A single layer DEA with failures, including cracks and short circuit.

C

Measurement

Figure C.1(a) and C.1(b) show the electrical results of a printed DEA. Figure C.1(a) shows the resistance between the bottom and the top electrodes is 71.4 kΩ; Figure C.1(b) shows the resistance of the top electrode is 14.8 Ω. Consequently, the bottom and the top conductive electrodes are electrically and mechanically isolated.

(a) (b)

Figure C.1. Observations of a DEA on the electrical performance. (a) Resistance measurement between the bottom and the top electrodes. (b) Resistance measurement of the top silver electrodes.

The thickness measurement of the PDMS layer is done by using SEM. The sample was cut in half; therefore, extra samples were required. The black tape on the lower part in Figure C.2 is the conductive tape for attaching the sample to the holding table.
Figure C.3 shows how the actuator is clamped/attached vertically to the clamp. A laser sensing module points at the tip of the cantilever beam part of the DEA. The actuator is facing back to the laser sensor, which means the actuator will bend towards the sensor during the actuation. The two contact pads are attached to the two red wires to the power supply.
To further validate the characterization of DEA and provide intuitive curve graphics, the lined-up frequency response plot was presented in Figure C.4. It is the curve version of the scatter Bode plot, which was shown in Figure 3.16.

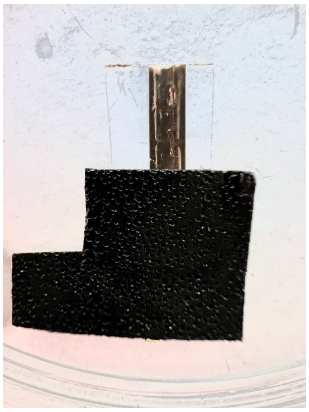

Figure C.2. Close-up of the sample that was used for polymer layer measurement after being cut and measured.

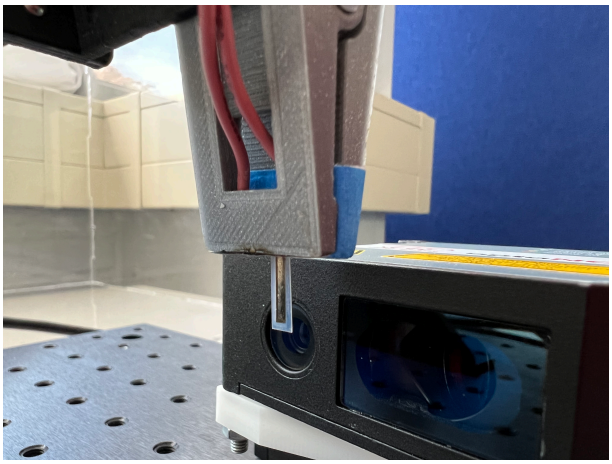

Figure C.3. The close-up of the DEA being clamped on a clip and tested with power on.

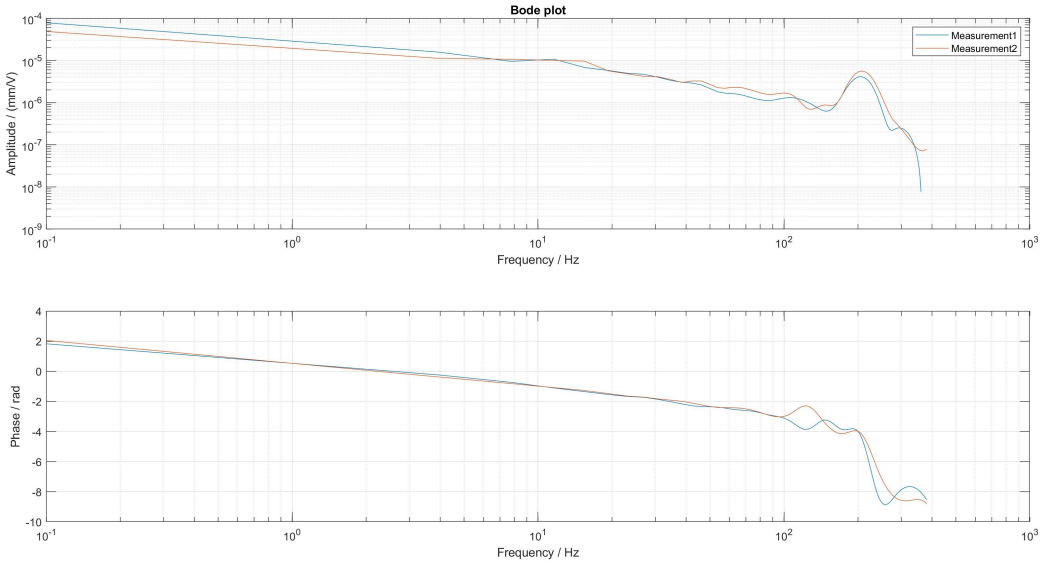

Figure C.4. The Bode plot of a fully inkjet printed DEA.

References

[1] Y. Wang and J. Zhu, “Artificial muscles for jaw movements,” *Extreme Mechanics Letters*, vol. 6, pp. 88–95, 2016. [Online]. Available: https://www.sciencedirect.com/science/article/pii/S2352431615300298.

[2] L. Li, H. Godaba, H. Ren, and J. Zhu, “Bioinspired soft actuators for eyeball motions in humanoid robots,” *IEEE/ASME Transactions on Mechatronics*, vol. 24, no. 1, pp. 100–108, 2019.

[3] A. O’Halloran, F. O’Malley, and P. McHugh, “A review on dielectric elastomer actuators, technology, applications, and challenges,” *Journal of Applied Physics*, vol. 104, 2008.

[4] W.-G. Drossel, H. Kunze, A. Bucht, L. Weisheit, and K. Pagel, “Smart3 – smart materials for smart applications,” *Procedia CIRP*, vol. 36, pp. 211–216, 2015, CIRP 25th Design Conference Innovative Product Creation, ISSN: 2212-8271. DOI: https://doi.org/10.1016/j.procir.2015.01.055. [Online]. Available: https://www.sciencedirect.com/science/article/pii/S2212827115004291.

[5] P. Brochu and Q. Pei, “Dielectric elastomers for actuators and artificial muscles,” in *Electroactivity in Polymeric Materials*, L. Rasmussen, Ed. Boston, MA: Springer US, 2012, pp. 1–56, ISBN: 978-1-4614-0878-9. [Online]. Available: https://doi.org/10.1007/978-1-4614-0878-9_1.

[6] J.-H. Youn, S. M. Jeong, G. Hwang, *et al.*, “Dielectric elastomer actuator for soft robotics applications and challenges,” *Applied Sciences*, vol. 10, no. 2, 2020, ISSN: 2076-3417. [Online]. Available: https://www.mdpi.com/2076-3417/10/2/640.

[7] A. Poulin, S. Rosset, and H. R. Shea, “Printing low-voltage dielectric elastomer actuators,” *Applied Physics Letters*, vol. 107, 24 Dec. 2015, ISSN: 00036951. DOI: 10.1063/1.4937735.

[8] Y. Kawahara, S. Hodges, B. S. Cook, C. Zhang, and G. D. Abowd, “Instant inkjet circuits: Lab-based inkjet printing to support rapid prototyping of ubicomp devices,” in *Proceedings of the 2013 ACM International Joint Conference on Pervasive and Ubiquitous Computing*, ser. UbiComp ’13, Zurich, Switzerland: Association for Computing Machinery, 2013, pp. 363–372, ISBN: 9781450317702. DOI: 10.1145/2493432.2493486. [Online]. Available: https://doi-org.tudelft.idm.oclc.org/10.1145/2493432.2493486.

[9] E. Hamad, S. Bilatto, N. Adly, *et al.*, “Inkjet printing of uv-curable adhesive and dielectric inks for microfluidic devices,” *Lab Chip*, vol. 16, Dec. 2015. DOI: 10.1039/C5LC01195G.

[10] N. Komuro, S. Takaki, K. Suzuki, and D. Citterio, “Inkjet printed (bio)chemical sensing devices,” *Analytical and bioanalytical chemistry*, vol. 405, May 2013. DOI: 10.1007/s00216-013-7013-z.

[11] J. Wu, R. Roberts, N. Tien, and D. Li, “Inkjet printed silver patterning on pdms to fabricate microelectrodes for microfluidic sensing,” vol. 2014, Nov. 2014. DOI: 10.1109/ICSENS.2014.6985197.

[12] P. Lotz, M. Matysek, and H. F. Schlaak, “Fabrication and application of miniaturized dielectric elastomer stack actuators,” *IEEE/ASME Transactions on Mechatronics*, vol. 16, pp. 58–66, 1 Feb. 2011, ISSN: 10834435.

[13] C. T. Nguyen, H. Phung, T. D. Nguyen, *et al.*, “A small biomimetic quadruped robot driven by multistacked dielectric elastomer actuators,” *Smart Materials and Structures*, vol. 23, 6 2014, ISSN: 1361665X.

[14] O. A. Araromi, A. T. Conn, C. S. Ling, J. M. Rossiter, R. Vaidyanathan, and S. C. Burgess, "Spray deposited multilayered dielectric elastomer actuators," *Sensors and Actuators, A: Physical*, vol. 167, pp. 459–467, 2011.

[15] F. Carpi and D. D. Rossi, "Contractile folded dielectric elastomer actuators," vol. 6524, SPIE, Apr. 2007, p. 65240D, ISBN: 081946645X.

[16] S. Elschot, "Inkjet printing of a low actuation voltage dielectric elastomer actuator," 2021. [Online]. Available: http://repository.tudelft.nl/..

[17] H. Shigemune, S. Sugano, J. Nishitani, *et al.*, "Dielectric elastomer actuators with carbon nanotube electrodes painted with a soft brush," *Actuators*, vol. 7, no. 3, 2018, ISSN: 2076-0825. [Online]. Available: https://www.mdpi.com/2076-0825/7/3/51.

[18] G. Kovacs, L. Düring, S. Michel, and G. Terrasi, "Stacked dielectric elastomer actuator for tensile force transmission," *Sensors and Actuators A: Physical*, vol. 155, no. 2, pp. 299–307, 2009, ISSN: 0924-4247. [Online]. Available: https://www.sciencedirect.com/science/article/pii/S0924424709004002.

[19] G.-K. Lau, S. C.-K. Goh, and L.-L. Shiau, "Dielectric elastomer unimorph using flexible electrodes of electrolessly deposited (eld) silver," *Sensors and Actuators A: Physical*, vol. 169, no. 1, pp. 234–241, 2011, ISSN: 0924-4247. [Online]. Available: https://www.sciencedirect.com/science/article/pii/S0924424711002846.

[20] DowInc., "Sylgard™ 184 silicone elastomer kit | dow inc.," 2022. [Online]. Available: https://www.dow.com/en-us/pdp.sylgard-184-silicone-elastomer-kit.01064291z.html.

[21] SigmaAldrich, "Safety data sheet," 2022. [Online]. Available: https://www.sigmaaldrich.com/NL/en/sds/ALDRICH/W280607.

[22] MitsubishiImagingInc., "Nbsij-mu01 safety data sheet," 2020. [Online]. Available: http://www.mitsubishiimaging.com/support/SDS/NBSIJ-MU01.pdf.

[23] Novacentrix, "Js-a211 data sheet," 2020. [Online]. Available: https://www.novacentrix.com/datasheet/Metalon-JS-A211-TDS.pdf.

[24] SussMicroTec, "Lp50 inkjet printer," 2022. [Online]. Available: https://www.suss.com/en/products-solutions/inkjet-printing/lp50.

[25] "Operating instructions optoncdt 1750." [Online]. Available: www.micro-epsilon.com.

[26] "Usb-6211 multifunction i/o device." [Online]. Available: https://www.ni.com/nl-nl/support/model.usb-6211.html.

[27] "Version2.0 august2021 hva1500/50 user manual."

[28] I. Koch, "Reduce charging in sem using low voltage imaging." [Online]. Available: https://www.nanoscience.com/applications/materials-science/reduce-charging-in-sem-using-low-voltage-imaging/.

[29] S. Magdassi, *The chemistry of inkjet inks*. World scientific, 2009.

[30] B. Derby, "Inkjet printing of functional and structural materials: Fluid property requirements, feature stability, and resolution," *Annual Review of Materials Research*, vol. 40, pp. 395–414, 2010, ISSN: 15317331. DOI: 10.1146/annurev-matsci-070909-104502.

[31] D. Jang, D. Kim, and J. Moon, "Influence of fluid physical properties on ink-jet printability," *Langmuir*, vol. 25, no. 5, pp. 2629–2635, 2009, PMID: 19196020. DOI: 10.1021/la900059m. eprint: https://doi.org/10.1021/la900059m. [Online]. Available: https://doi.org/10.1021/la900059m.

[32] R. Mikkonen, P. Puistola, I. Jönkkäri, and M. Mäntysalo, "Inkjet printable polydimethylsiloxane for all-inkjet-printed multilayered soft electrical applications," *ACS Applied Materials and Interfaces*, vol. 12, pp. 11 990–11 997, 10 Mar. 2020, ISSN: 19448252. DOI: 10.1021/acsami.9b19632.

[33] J. Y. Park, H. Y. Chae, C. H. Chung, *et al.*, “Controlled wavelength reduction in surface wrinkling of poly(dimethylsiloxane),” *Soft Matter*, vol. 6, pp. 677–684, 3 2010, ISSN: 1744683X. DOI: 10.1039/B916603C.

[34] J. S. Kang, H. S. Kim, J. Ryu, H. T. Hahn, S. Jang, and J. W. Joung, “Inkjet printed electronics using copper nanoparticle ink,” *Journal of Materials Science: Materials in Electronics*, vol. 21, pp. 1213–1220, 11 Nov. 2010, ISSN: 09574522. DOI: 10.1007/s10854-009-0049-3.

[35] F. Dimatix, “Frequently asked questions - dimatix materials printer and cartridge,” 2020.